UNIVERSITÀ DEGLI STUDI
DI MILANO

**PHD IN TRANSLATIONAL MEDICINE**

Department of Biomedical Sciences for Health

XXXIV CYCLE

PhD Thesis

# Cell Penetrating peptide-conjugated Morpholino: a novel compound to rescue SMA in a symptomatic phase

Margherita Bersani

R12329

TUTOR: Prof.ssa Stefania Paola CORTI

COORDINATOR: Prof.ssa Chiarella SFORZA

A.Y. 2020/2021

# ABSTRACT

Spinal muscular atrophy (SMA) is a motor neuron disease and the leading genetic cause of infant mortality. Recently approved SMA therapies have transformed a deadly disease into a survivable one, but these drugs show effective rescue only in the early stages of the disease. Therefore, safe, symptomatic-suitable, non-invasive treatments effective across different phenotypes are urgently needed. In the past three years, we used morpholino (MO) chemistry to conjugate antisense oligonucleotides that increase SMN protein levels to cell-penetrating peptides (CPPs) for better cellular distribution. Systemically administered MOs linked to r6 and (RXRRBR)2XB peptides were able to cross the blood-brain barrier and to increase SMN protein levels remarkably, causing striking improvement of survival, neuromuscular function, and neuropathology, even in symptomatic SMA animals. This study demonstrates that MO-CPP conjugates can significantly expand the therapeutic window through minimally invasive systemic administration, making it a good candidate for clinical application.

# TABLE OF CONTENTS

# 1. INTRODUCTION

## 1.1. Spinal Muscular Atrophy (SMA)

Spinal muscular atrophies (SMAs) are a group of hereditary autosomal recessive disorders characterized by early age of onset and selective degeneration of α-motor neurons (MNs) in spinal cord and brainstem. Because of this loss, patients affected by these diseases show a progressive proximal muscle weakness, hyposthenia and paralysis.

These atrophies show a great variability of clinical features, like age of onset and severity of the disease.

The most common form, which belongs to Proximal Muscular Atrophy with childhood onset, is an autosomal recessive disease (SMA5q, OMIM #253300) with an incidence of 1 in 6000 to 1 in 10000 live births, with a carrier frequency of 1/40-1/60 60 [1]. The genetic cause is a mutation or homozygous deletion in the telomeric copy of SMN (Survival Motor Neuron) gene (SMN1), on 5q chromosome, which causes a depletion of SMN protein [2].

The term SMA is often used to indicate the most common form among these pathologies (SMA5q) and in this sense it will be also used in this work. The typical clinical aspects present in SMA5q are generalized muscle weakness and atrophy; the pathology is characterized by a progressive and symmetrical muscle involvement, weakness and atrophy resulting in the loss of voluntary control of limbs and trunk movements, postural, swallowing and breathing. The intellectual functions remain the same and there is no involvement of sensory neurons [2].

The analysis of patients' tissues shows evident signs of gliosis in the anterior horn of the spinal cord and reduction in motor neurons number. Surviving

motor neurons show both signs of degeneration, suggesting an ongoing process of neuronal death, and signs of immaturity: they have a small size, are pyknotic, and have the Nissl substance poorly developed [3]. Axons analysis at the level of the ventral roots show fasciculations convoluted by a single Schwann cell, a lower density and a high percentage of poorly myelinated axons, while in the neuromuscular junctions are found neurofilaments aggregates at the presynaptic level. Muscle endplates are smaller, immature and sometimes denervated [4]; muscle biopsy in infants shows large groups of atrophic fibers interspersed with fascicles of hypertrophied and normal fibers [5].

## 1.2. Clinical classification

SMA is clinically classified into four groups, according to the age of onset and the severity of motor dysfunctions of affected subjects (**Table 1**). A fifth group (type 0) has been added to describe a severe form characterized by pre-natal onset and death within 3 weeks after birth [6].

| SMA TYPE | AGE OF ONSET | HIGHEST MOTOR FUNCTION ACHIEVED | LIFE EXPECTANCY |
|---|---|---|---|
| **Type 0** | Pre-natal | None | Less than 1 month |
| **Type I** | 0-6 months | Never sit unassisted | Less than 2 years |
| **Type II** | 7-18 months | Can sit unassisted | Between 2 years and 4 years |

| | | | |
|---|---|---|---|
| **Type III** | After 18 months | Can stand and walk unaided | Normal life expectancy |
| **Type IV** | Second or third decade | Can stand and walk unaided | Normal life expectancy |

**Table 1**: Clinical classification of SMA

This classification brought several clinical advantages, even though SMA patients do not have all the characteristics typical of a specific phenotype, so prognostic information cannot be always extrapolated.

- **Type 0:** severe form characterized by pre-natal onset and death within 3 weeks of age.
- **Type I**: named Werdnig- Hoffman disease, is the most common and severe form. Infants never gain the ability to sit unsupported. The head control is usually missing.
- **Type II**: named Dubowitz Disease, is the intermediate chronic infantile onset form. Affected children reach the ability to sit without any support and some of them could be stand, although they cannot walk.
- **Type III**: named Wohlfart-Kugelberg-Welander disease, is the mild chronic juvenile onset form. Patients reach the ability to walk unaided, and some of them could never need wheelchair assistance during childhood.
- **Type IV**: is the adult onset form. Patients have the ability to walk and no problems related with respiration and nutrition are observed.

## 1.3. *SMN1* and *SMN2*

The causative gene of SMA was mapped in 1990 in a complex region of chromosome 5q (5q11.2-13.2) which contains an inverted duplication. This region is mapped by the Survival Motor Neuron (SMN) gene, that was then identified as responsible for the disease [7]. In the human genome, there are two almost identical SMN gene on chromosome 5q13: the telomeric or *SMN1* gene, which is SMA causative gene, and the centromeric one, *SMN2* (Figure 1).

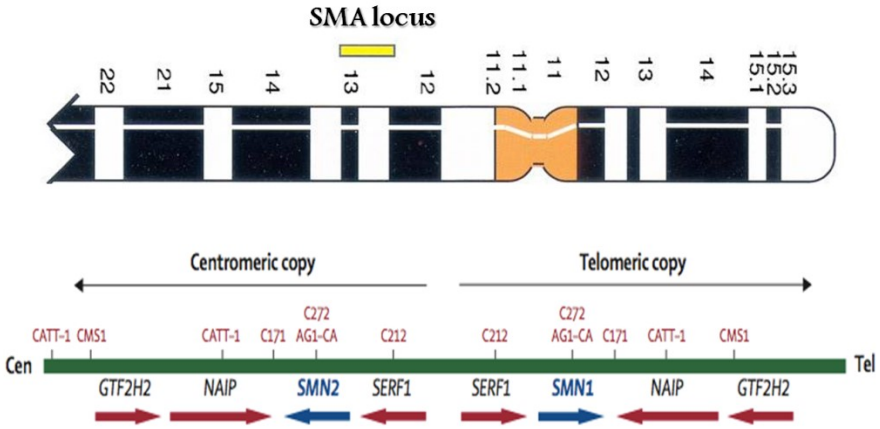


**Figure 1**: Locus of SMA causative gene, *Survival Motor Neuron (SMN)*, localized in a complex region of chromosome 5q (5q11.2-13.2) including many modifiers genes like *General Transcription Factor IIH (GTF2H2), Neuronal Apoptosis Inhibitory Protein (NAIP), Small EDRK-Rich Factor 1(SERF1)*[8]

*SMN* is composed of nine exons (exon 1, 2a, 2b, 3-8) and eight introns and it covers a genomic region of about 20 kb. The difference between the sequence of the two genes is the substitution of only 5 nucleotides (Figure 2), of which one is located in the coding region of the gene [9].

The *SMN1* gene encodes a homonymous 38 KDa of 294 aminoacids which is ubiquitously expressed in human somatic tissues. It is very likely the

hypothesis that while *SMN1* gene is highly conserved in species from yeast to man, *SMN2* gene is only found in the human genome [10].

The severity of the disease phenotype is mainly related to the number of copies of *SMN2* found in patient's genome; in fact, the majority of patients have an homozygous mutation, rearrangement or deletion in the *SMN1* gene, but at least one copy of *SMN2* gene [11]. Two copies of *SMN2* determine SMA type I, three copies determine SMA type II and three or four copies of *SMN2* determine SMA type III or IV [12]. Patients with more than 5 copies of *SMN2* show no sign of SMA even if they lack *SMN1* [13]. This is due to the fact that about 10% of full-length transcripts are produced by every copy of *SMN2*, and consequently the increased expression of protein SMN-FL comes from *SMN2* gene, which is a benefit for patients.

As a gene, *SMN2* is subjected to alternative splicing, which occurs after the transcription. The alternative splicing of *SMN2* pre-mRNA produces an mRNA lacking of exon 7 or, rarely, exon 5. The exclusion of exon 7 from the mRNA of *SMN2* is caused by a single C>T replacement in position +6 of this exon [14]. Despite being a silent mutation, which does not alter the amino acid sequence of the translated protein, it is localized at the level of an exonic splicing enhancer and therefore removes exon 7 during the transcription. In 2002, Cartegni and Kranier supported the hypothesis that the substitution C>T in exon 7 alters the sequence of an Exonic Splicing Enhancer (ESEs), suppressing its function. The exon 7 of *SMN* gene is characterized by a weak splice site 3'. The inclusion of exon 7 in mRNA is positively regulated by many exonic factors in cis, called intronic splicing enhancer, while it is negative regulated by exonic elements in cis called Exonic Splicing Silencers (ESSs) or Intronic Silencers (ISSs). All of these cis elements (Figure 2) are recognized by transacting splicing proteins rich in serine-arginine (SR

proteins) and several heterogeneous nuclear ribonucleoprotein (hnRNPs) [15].

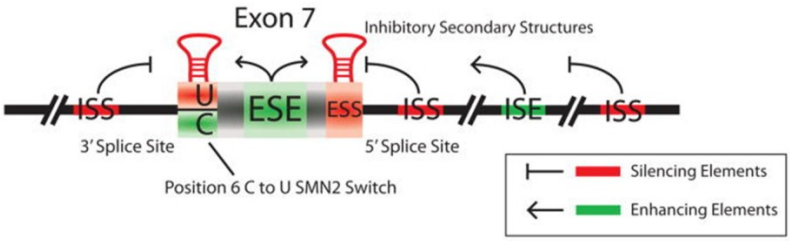


**Figure 2**: Splicing architecture of exon 7 of SMN gene: multiple RNA elements influence alternative exon 7 recognition [8].

In exon 7, the exonic splicing enhancer binds the Splicing Factor 2 (SF2), also named alternative splicing factor (ASF). SF2, in order to form the splicing complex involved in the intron 7 removal from *SMN1* pre-mRNA, binds in turn the U2 class of small nuclear ribonuclear protein (U2 snRNP) and the U2 auxiliar factor (U2AF).

A second hypothesis proposed in 2003 by Kashima and Manley argued that the substitution C > T in *SMN2* generates an ESS that, tying hnRNP A1, facilitates the exon 7 skipping. This theory is supported by the knockdown of hnRNP A1 by siRNA (small interfering RNA) which induces an increase in exon 7 inclusion. These two models are not necessarily incompatible and a third hypothesis, joining the two above-mentioned mechanisms, explains the alternative splicing of *SMN* transcript in a dual mechanism that includes both the loss of a specific ESE for SF2/ASF and the simultaneous creation of a specific ESS for hnRNP A1[16]. The most important intronic splicing regulator of introns 6 and 7 is ISS- N1 which exerts a powerful effect on the activity of other positive elements in cis of exon 7 and intron 7. Antisense oligonucleotides against ISS- N1 determine the inclusion of exon 7 in almost all *SMN2* mRNA transcripts [17].

According to another study, an exonic splicing suppressor promotes the binding of heterogeneous nuclear ribonuclear protein A1 (hnRNP A1) or splicing suppressor protein, and sterically hamper the formation of the splicing complex or its stabilization [18]. Even if the two hypotheses have been tested, the exact mechanism of the exon 7 exclusion remains unsolved (Figure 3).

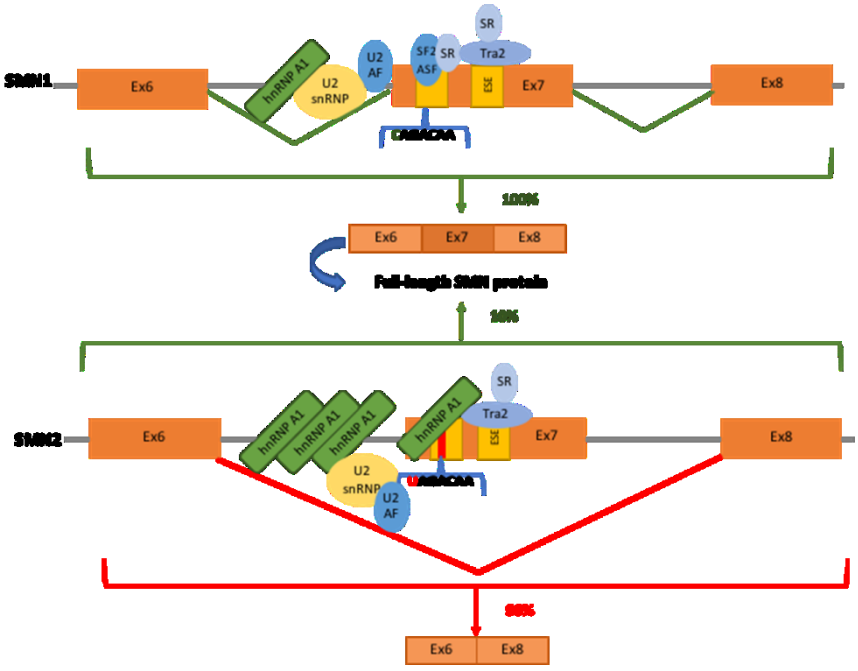


**Figure 3**: Alternative splicing process of the *SMN1* and *SMN2* pre-mRNAs. The C6T substitution within *SMN2* causes the removal of exon7 from about 90% of the *SMN2* mRNAs [18].

Despite the different mechanism, *SMN1* gene produces a transcript full-length (FL) that undergoes to a correct splicing in almost 100% of cases, while the *SMN2* produces only 10% of the transcript FL and in 90% of cases produces

a transcript missing exon 7 (SMNΔ7). The full length mRNA *SMN1* and *SMN2* genes coding for identical proteins of 294 amino acids, while the transcript missing exon 7 (isoform SMNΔ7) encoding for a truncated protein of 282 aa which is unstable and has a reduced ability to oligomerization; this results in a lower functionality of the protein and an early degradation [19] (Figure 4).

*SMN2* gene produces only a small fraction of functional SMN protein than its homologous telomeric counterpart, insufficient for normal survival of motor neurons [2].

Ever since SMN protein was identified as the direct cause of SMA, many studies investigated the molecular functions of this ubiquitously expressed protein. SMN was demonstrated to be present at the leading edge of neurite outgrowths in mouse embryonal teratocarcinoma cells, suggesting that SMN may play a role in this process. In addition, SMN was detected within the cytoplasm of skeletal muscle during the first 2 weeks after birth and in neuro muscular junctions (NMJs). Taken together, these results suggest that SMN may indeed fulfill neuronal- and muscle-specific functions (Fan 2002). SMN also seems to play important roles in mRNA trafficking and local translation and cytoskeletal dynamics [20]. There are two main hypotheses to link the lack of SMN protein and the MN degeneration. The first one involves the impairment of the snRNPs complex: when the normal splicing does not occur, the functions and survival of MNs are compromised. It has been demonstrated that when the levels of SMN protein are low, there is a lack of U11 and U12 snRNPs which constitute the minor spliceasome, responsible for the splicing of a minority of introns [21]. Some of them are mainly expressed in the nervous system and encode for essential neuronal component, like synaptic components and voltage gated ion channels.

The second hypothesis is based on the specific role that SMN protein could have for MNs, such as mRNA transport along the axons [22]. This protein protein seems to be involved in the membrane remodeling of MNs, which is very specialized for its extreme polarity, for the extension of the cellular processes and for the presence of NMJs. These data suggest that SMN is involved in MNs function and viability through the regulation of axonal transport, the remodelling of membrane domains and the preservation of NMJs' structural activity.

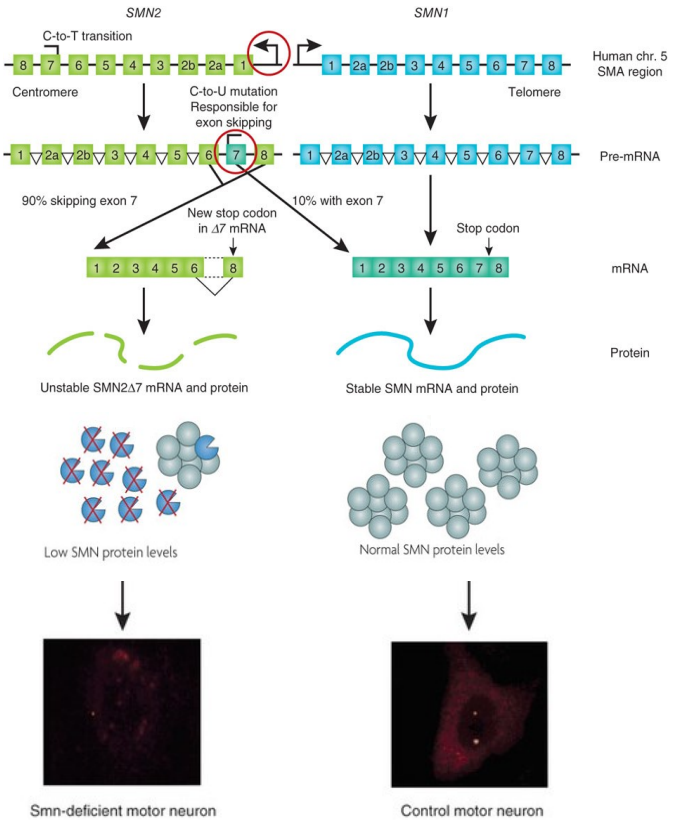

**Figure 4**: The Survival Motor Neuron Genes *SMN1* and *SMN2* have an identical structure and are 99.9% identical at the sequence level. The difference between the two genes is a single-nucleotide change in exon 7 (C or T). This single nucleotide change affects the splicing of the gene, so most SMN transcripts from *SMN2* lack exon 7, whereas those from *SMN1* contain exon 7. The loss of the amino acids that are encoded by exon 7 results in the production of an SMN protein with severely decreased oligomerization efficiency and stability, and the SMN monomers are rapidly degraded. In a minority of cases, *SMN2* transcripts contain exon 7 and encode for a normal, full-length SMN protein.

## 1.4. Animal Models for SMA

### 1.4.1. Murine models for SMA

As already mentioned, murine model represents the closer model to the human pathology and more useful for the clinical research. In nature, mice harbor only one copy of the survival motor neuron gene, *Smn1*. If *Smn1* gene is disrupted in homozygosis, a failure of early development of mice embryos occurs, leading to pre-natal death [23]. Different models have been produced adding to a *Smn1* knockout different copies of the human *SMN2* to rescue the lethal phenotype and produce SMA models with different level of disease severity (**Table 2**).

The first murine model produced for SMA was FVB.Cg-Smn1tm1Hung Tg(SMN2)2Hung/J, called also the Hung-Li SMA mice (Jackson laboratory stock #005058). It has a homozygous null mutation in the murine *Smn* gene and carries a full-length human SMN2 transgene [24], and it is used as a model for SMA type II.

Successively, another mouse model was developed by Monani et al.: SMN1A2G, which resembles SMA type III in humans by carrying a *SMN1* transgene with A2G missense mutation [25].

The most widely used SMA model is Δ7 SMA mice [26].

| Model Name | Genotype | SMA type | Life expectancy | Phenotype |
|---|---|---|---|---|
| **Smn1 null mutation** | Smn -/- | Type I | Pre-natal mortality | Severe |
| **Hung-Li mouse** | Smn1hung-/-;SMN2Hungtg/- | Type II | 13 days | Intermediate: Similar to the Δ7 mouse model. |
| **Δ7 mouse model** | The Smn1-/-; SMN2tg/tg;SMNΔ7tg/tg | Type II | 13 days | Intermediate: Muscle weakness is present from P5 and progress over time, abnormal gait, tendency to fall. ByP9 around 50% of LMNs are lost. |
| **A2G mouse** | The Smn1-/-; SMN2tg/tg;SMN1A2G | Type III | Less than 1year | Mild: Milder than the Δ7 mouse. Decreased body weight, muscle atrophy and weakness. |

**Table 2**: different mouse models for SMA

### 1.4.2. Δ7 SMA mice

The most commonly used SMA animal models is the FVB.Cg-Grm7Tg(SMN2)89Ahmb Smn1tm1Msd Tg(SMN2*delta7)4299Ahmb/J, the so called Δ7 SMA mice (Jackson Laboratory stock #005025).

The model used in this work is called Δ7 SMA mice. The first SMA model produced derived from a knockout background for *Smn1* to whom was added one entire *SMN2* transgene (*Smn1−/−; SMN2+/+*) expressing full-length SMN protein under the control of the human *SMN2* promoter. This model resembles the human SMA patients' condition, where there is only a moderate amount of SMN produced by the remaining *SMN2* gene. It is considered a

model for type I SMA. Then, to obtain a less severe model for SMA type I/II, another transgene containing a human *SMN2* cDNA without exon 7 (SMNΔ7) was added to this strain. This resulted in a triple homozygous mice, that was defined as the Δ7 SMA mice (Smn-/-; SMN2+/+; SMNΔ7+/+) [27]. The first difference to be observed in SMNΔ7 mice and healthy mice at birth is body weight, significantly lower. SMNΔ7 mice start to be symptomatic from P5 and the first sign is their inability to right themselves if place on their backs. At P10 they show important difficulty in ambulating and walking, with a tendency to fall over. They also have strong muscle weakness of the hindlimbs, that they show at this time point, and an abnormal gait and shakiness (fibrillation) during walking. The mean survival of SMNΔ7 mice is ∼13 days [27].

## 1.5. Therapeutic approaches and clinical issues

The majority of therapies for SMA are focused on increasing SMN protein production, using exon splicing on *SMN2* or carrying a wild-type copy of *SMN1*. The currently FDA approved therapies are the following.

### Nusinersen

The approach that first obtained the FDA approval in 2016 – and EMA's in 2017- is based on antisense oligonucleotide (ASO) technology: nusinersen, marketed as Spinraza by Biogen, is a 18-mer length modified ASO with phosphorothioate linkages that targets the intronic splicing silencer N1 (ISS-N1) located in the intronic sequence downstream exon 7 in SMN2 gene (Figure 5) [28]. While waiting for regulatory approval, nusinersen was made available for compassionate use for SMA type I infants by the pharmaceutical

company. This approval and commercialization were supported by several trials demonstrating efficacy without any major drug-related adverse event. After promising results for nusinersen in phase I and II trials in children with SMA type II and III, two phase III, randomized, double-blind, sham-procedure controlled studies were initiated consequently. ENDEAR (ClinicalTrials.gov identifier: NCT02193074) assessed safety and clinical efficacy of nusinersen in 121 infants with infantile-onset SMA and younger than seven months. In the interim analysis, infants treated with nusinersen had higher improvement in motor functions than controls. Moreover, the nusinersen group demonstrated a prolonged time to death or need for permanent ventilation compared to controls. Furthermore,infants with shorter disease duration at screening had better response to treatment [29].

CHERISH (ClinicalTrials.gov identifier: NCT0229253) involved 126 children with later-onset SMA. In the final analysis, 57% of nusinersen patients vs. 26% in the sham group had a rise of three points in motor function scores after 15 months of treatment [29].

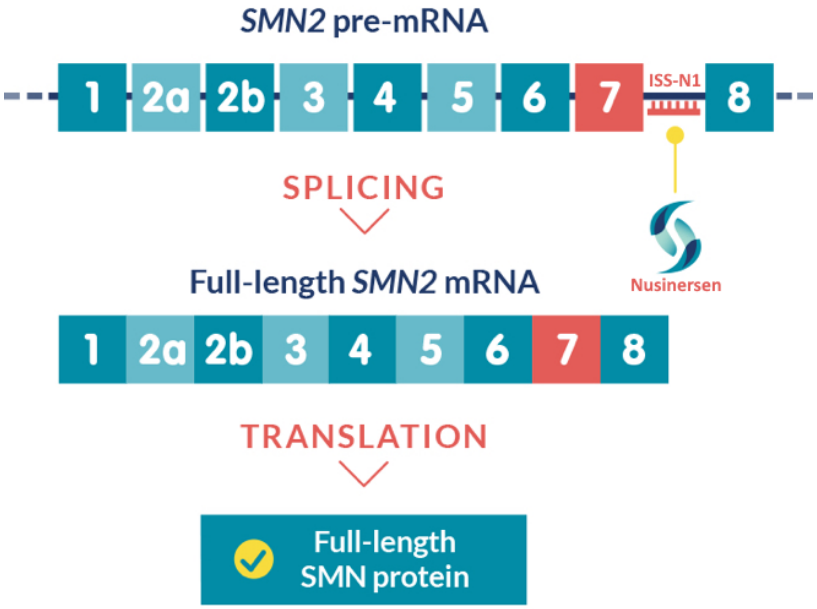


**Figure 5**: Nusinersen mechanism of action [30].

ASOs do not cross the blood-brain barrier, therefore the administration of Spinraza is currently performed by intrathecal injection, with recommended dosage of 12 mg per administration [29]. The treatment starts with 4 loading doses, the first 3 of which separated by intervals of 14 days. The last administration should be made 30 days after the third one. In the following maintenance phase the administrations are made once every 4 months. The distribution of the drug into the cerebrospinal fluid, MNs, glia and vascular endothelial cells, with a mean time of elimination of 135-177 days, was demonstrated. Then the drug reaches the systemic circulation, where it remains up to 80 days, and lastly it is cleared by kidney, liver and skeletal muscle as seen at autopsy [31]. Even if the approval of nusinersen brought a great improvement in SMA patients clinical management, intrathecal

administration happens to be difficult for patients who had surgeries for scoliosis; moreover, the lack of clinical trials on adults
at the time of approval and the few information regarding the dose still represent a problem [20]; by now, the evidence supports the necessity of a treatment as early as possible [32], and one of the clinical trials, the ENDEAR study, also highlighted that patients with longer disease duration had less benefit from nusinersen [29].

Zolgensma

Onasemnogene (Zolgensma), FDA approved in 2019, EMA 2020, is a non-replicating adeno-associated virus 9 (AAV9) designed to provide the wild-type copy of the gene encoding the human SMN protein [33].
Onasemnogene is approved for the treatment of only <2 years patients who have been diagnosed with SMA type 1 or have up to 3 copies of *SMN2* (EMA). It is administered in a single dose by intravenous infusion [33]. This construct, an AAV9 vector carrying SMN1 complementary recombinant DNA, can cross the brain–blood barrier, produces a sustained expression of SMN protein and prolongs survival of treated SMA-mice [29]. Clinical trials results showed a preserved respiratory function, improvement in motor functionality, higher survival and reduction of hospitalizations. The main advantages of this approach are that a one-time injection is needed and it would lead to systemic expression of the SMN protein, while a disadvantage could be the reported presence of pre-existing anti-AAV9 antibody in the SMA population [46].

Risdiplam

Risdiplam (Hoffmann-La Roche) is a small molecule with a *SMN2* pre-mRNA splicing modifier role. It has higher specificity toward SMN2 compared to the other standard splicing modifier. Another positive aspect of Risdiplam is the oral non-invasive route of administration. It is able to reach both CNS and peripheral organs. In vitro and in vivo preclinical studies demonstrated the ability of the compound of strongly increase the amount of functional full length SMN protein in blood, central nervous system, muscles and other peripheral tissues, with a wide biodistribution of Risdiplam [29].
Risdiplam was approved in 2020 by FDA and in 2021 by EMA for 2-months and older patients with a clinical diagnosis of SMA Type 1, Type 2 or Type 3 or with one to four SMN2 copies [34].

### 1.5.1. SMN-independent therapies

In addition to the SMN-targeting therapies already approved by FDA, there are also different approaches defined as SMN-independent strategies, sometimes suggested to be combined to SMN-targeting strategies. The association could allow the complete restoration of the phenotype, ability that targeting *SMN* in some cases is are not able to perform. Here are the most promising SMN-independent treatments under evaluation.

Olesoxime

Olesoxime (TRO19622, Hoffmall-La Roche) is a cholesterol-like compound that performs a neuroprotective role by targeting two proteins of the outer mitochondrial membrane implicated into the control of the mitochondrial permeability transition pore. It was discovered for its neuroprotective ability into preventing MN loss in a trophic factor deprived environment and for its neuroregenerative effects in *in vivo* model of motor nerve degeneration. Its

mechanism of action is based on the prevention of excessive mitochondrial permeability, resulting in reduced production of reactive oxygen species (ROS), inhibition of pro-apoptotic factor release and maintenance of the mitochondrial energetic production [35]. The effects registered in clinical trials are not meaningful enough to be approved by FDA, but it was seen that Olesoxime can slow the motor decline of the pathology and thus suggested its possible use in combination with SMN-targeting therapies. Up to now, Roche has stopped the development of this product.

Plastin 3

In rare cases, SMA affected individuals are asymptomatic despite carrying the same *SMN1* mutations as their affected siblings, suggesting the existence of modifier genes. In 2008, Oprea et al, discovered that unaffected *SMN1*-deleted females exhibited significantly higher expression of *plastin 3* (*PLS3*) than their SMA-affected counterparts [36]. The group observed that *PLS3* was highly expressed in the human fetal and adult spinal cord, and in rat pheochromocytoma 12 (PC12) cells, *Pls3* expression significantly increased during neuronal differentiation, suggesting a role for Pls3 in this process. *PLS3* is important for axonogenesis through increasing the F-actin level, and overexpression of PLS3 rescues the axon length and outgrowth defects associated with SMN down-regulation in motor neurons of SMA mouse: *in vitro* experiments demonstrated that SMA MNs exhibited a significant reduction in axon length compared with cells from either WT or heterozygous embryos, and detrimental effect of a reduced *SMN* level on axonal length was significantly rescued by *PLS3* overexpression, axons reaching lengths comparable to WT and heterozygous embryos. Moreover, *PLS3* overexpression in zebrafish embryos revealed a slight but nonsignificant

increase in mild and moderate axon defects compared with controls, while the co-injection of *smn*-MO and *PLS3* RNA significantly rescued the aberrant axonal outgrowth in comparison with *smn* MO alone, suggesting that PLS3 plays a modifying role in the zebrafish SMA model as well [36].

Neurocalcin delta

*Neurocalcin delta* (*NCALD*), which encodes a neuronal calcium sensor protein, as an SMA-protective modifier in humans, acts as a negative regulator of endocytosis, which is in contrast to PLS3 acting as its positive regulator. Riessland et al. showed Ca-dependent interaction of NCALD with clathrin, a protein essential in endocytic vesicles coating, and demonstrated that low SMN levels reduced voltage-dependent Ca influx and that NCALD bound clathrin at low Ca levels, acting as a Ca-sensitive inhibitor of endocytosis [37]. Results obtained from multiple *in vitro* and *in vivo* experiments showed that NCALD suppression re-established synaptic function, most likely by restoring endocytosis. Interestingly, there are evidence that NCALD knockdown in various SMA animal models could ameliorate major functional SMA disturbances, such as motor axon development in zebrafish, or MN circuitry and presynaptic function of neuromuscular junction (NMJ) in mice. The work suggested that a combinatorial therapy that both elevated SMN and decreased NCALD may provide a full protection of SMA patients, resulting in asymptomatic individuals [37].

Calcineurin-like EF-hand protein 1

Calcineurin-like EF-hand protein 1 (CHP1) is a PLS3 interacting protein, as demonstrated by co-immunoprecipitation and pull-down assays [38].

Although CHP1 is ubiquitously present, it is particularly abundant in the central nervous system, MN growth cones and NMJs; elevated CHP1 levels were found in SMA mice. Congruently, CHP1 downregulation restored impaired axonal growth in Smn-depleted NSC34 MN-like cells, SMA zebrafish and primary murine SMA MNs [38].

Moreover, combined subcutaneous injection of low-dose SMN antisense oligonucleotide in pre-symptomatic mice and CHP1 reduction by genetic modification prolonged survival by 3.6-fold; CHP1 reduction also ameliorated SMA disease hallmarks including electrophysiological defects, smaller NMJ size, impaired maturity of NMJs and smaller muscle fibre size. There is evidence that CHP1 is a novel SMA modifier that directly interacts with PLS3, and that CHP1 reduction ameliorates SMA pathology by counteracting impaired endocytosis. CHP1 reduction can be considered a possible SMN-independent therapeutic target for a combinatorial SMA therapy [38].

Stem cell transplantation

A different approach could be the transplantation of corrected MNs derived from SMA-induced pluripotent stem cells (iPSCs) into the spinal cord of SMA mice. The procedure consists into producing iPSC reprogrammed cell lines from SMA patients' fibroblasts, that has to be genetically corrected by converting *SMN2* into *SMN1*, using oligodeoxynucleotides, and then differentiated in MNs. In SMA mice this treatment ameliorated the phenotype of the disease. The MNs number and size were not as high as non-SMA mice, but were increased respect the control. In addition, it was observed that also the endogenous MNs had an increase in size, suggesting the neuroprotective role of the transplantation [39].

### 1.5.2. Issues in clinical practice

For SMA, early treatment is essential despite the fact that the therapeutic window in humans has yet to be established. The different molecules already approved or currently under evaluation are being shown to be good therapeutic possibilities to treat SMA, but it is essential to realize and finalize the clinical trials in order to compare the safety and efficacy profiles of each molecule to the others and optimize their use in accordance to the patient clinical features. The timing of administration is of crucial importance and is closely linked to the time of diagnosis [40]. The most recent trials on Nusinersen suggest that early treatment maximize efficacy [20].

Another limitation to be taken into consideration is immunogenicity of AAV9-based therapies like Zolgensma. Often a prolonged contact with AAV9 virus elicits an immune response, not always noticeable clinically but results in creation of AAV9 antibodies. This fact makes any redosing of Zolgensma impossible. Moreover, around 50% of adults and a small percentage of children naturally have antibodies against AAV9 and cannot receive this gene therapy treatment - or any other treatment that uses AAV9 viruses. In addition, in 2019, the company disclosed adverse effects on spinal neurons in lab animals when the treatment was administered intrathecally [41]; moreover, acute hepatotoxicity and sensory neuron toxicity were reported in primates and piglets [29] and very few data are available for patients older than two years [42]. This underlying the strong need for non-toxic, efficient therapies suitable for all patients.

## 1.6. Morpholino Antisense Oligonucleotides

The ASO on which this work is based is an oligomer with Morpholino (MO) technology. MOs differ from nucleic acids ASOs, substituting the sugar backbone with a methylenemorpholine ring-based one. In addition, the intersubunit linkage between the MO rings is further modified with a non-ionic phosphorodiamidate linkage. This structure is defined a phosphorodiamidate morpholino (PMO). It exhibits low toxicity and good capability into binding RNA with a melting temperature higher than RNA, DNA or phosphorothioate-linked DNA [43,44]. MO's mechanism of action is based on a steric block, that hampers the mRNA translation. The length of MO oligomers is crucial for their function: Burghes and demonstrated that MOs' length is directly correlated to the efficiency in human SMA fibroblast [45]. Another characteristic that influences the efficacy of MO is the position of the target sequence within ISS-N1. The most consistent effect was achieved when targeting 8-35 base region of intron 7, and the optimal length turned out to be 25 mer (MO-10-34) [46].

Recently Nizzardo et al. investigated the use of a 25-nt PMO in SMAΔ7 mice. The compound targets the ISS-N1 10 to 34 region (thus named MO10-34) modulating SMN2 splicing. Using different protocols of administration (ICV, subcutaneous or combined) the work demonstrates the efficacy of this MO in SMAΔ7 mice. This treatment resulted in increased full length SMN level in the central nervous system and in the other organs, rescue of the pathological phenotype, improvement of the survival, restored level of some small nuclear RNAs normally deregulated in SMA and amelioration of NMJs morphology and muscle trophism [47]. Due to the good biodistribution and the lack of side effects, this work focuses on MO10-34, even if its effect need somehow to be

improved: recent works in fact demonstrated that MO action can be enhanced either with small molecules [48] or Cell penetrating Peptides (CPPs) [49]. It is not the first time that a MO-based therapy is developed: the approval by FDA arrived in 2016 for Duchenne muscular dystrophy (DMD). It consists in a synthetic MO-based ASO named Eteplirsen. It mediates the skipping of the exon 51 of the dystrophin pre-mRNA restoring the reading frame of the RNA and thus stimulate the production of functional dystrophin (Baker 2017). Anyway, this approach showed limited efficacy too and thus need to be further improved. The use of Cell Penetrating Peptides (CPPs) is a possible solution.

## 1.7. Cell Penetrating Peptides (CPPs)

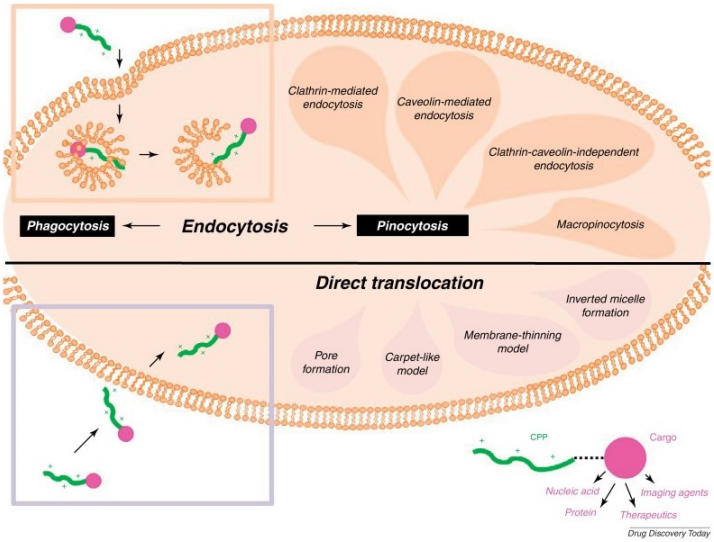


**Figure 6**. CPP internalization by different endocytic pathway and direct translocation [50]

To improve ASOs therapy and biodistribution, in this work we tested the conjugation with Cell Penetrating Peptides (CPPs). CPPs are a group of peptides, long up to 30 amino acids, able to transport across cellular

membranes different kind of cargoes as peptides, proteins, nucleic acids (siRNA, plasmid DNA, ASOs), liposomes and small drugs [51]. CPPs are internalized into the cells by different kind of endocytosis (clathrin- and caveolae-mediated endocytosis and micropinocytosis) showed in Figure 6, then released to the next extracellular space [52].

On the basis of their physicochemical properties CPPs can be divided in three classes [53]:

- Cationic CPPs: the majority of the CPPs have a net-positive charge at physiological pH. They contain a variable number of positive charged amino acids as arginine and lysine. The guanidine groups present in the arginine residues interact with the cell membrane lipids by electrostatic interactions and enter the cell by macropinocytosis.
- Amphipathic CPPs: amphipathic CPPs are mostly synthetic or chimeric peptides which contains hydrophobic amino acids as valine, leucine, isoleucine or alanine. The internalization mechanism is completely mediated by the hydrophobic region.
- Hydrophobic CPPs: hydrophobic CPPs have a low net charge and are composed only by nonpolar amino acids.

The most used CPPs are the following:

- pTat (GRKKRRQRRRPPQ: one of the first discovered and studied CPP. It is a 11-amino acid long peptide, derived from HIV-1, and belongs to the group of cationic CPPs thanks to its richness in arginine residues [54]. In recent years,pTat has been demonstrated to have toxic effects [50].

- RXR ($(RXRRBR)_2XB$) belongs to the arginine-rich class of CPPs and thus to the cationic class of CPPs. The high number of the arginine residues is the key component for its ability into crossing membranes [51].
- Penetratin-1 or Antp (RQIKIWFQNRRMKWKK) is a peptide of 60 amino acids that belongs to the homeodomain of Antennapedia from Drosophila. It is considered a cationic CPP [55].
- Transportan (GWTLNSAGYLLG) is a 27 amino acids-long hydrophobic peptide. It is a chimeric CPP composed by a part of the neuropeptide galanin (N-end) and mastoparan (C-end) linked by a lysine [56].

CPPs represent for neuromuscular disorders, as SMA, a promising solution to improve the passage of the drug across the BBB and reach the target tissues. As many other compounds, MO can be covalently conjugated to CPPs at either end (5' or 3') resulting in peptide-conjugated MO. For MOs the conjugation is usually performed by a covalent amide linkage, and in the majority of the cases involves arginine-rich CPPs [57].

Regarding SMA, in 2016, Meijboom et al., obtained promising results using a Pip6a CPP conjugated to a MO targeting the ISS-N1 element on *SMN2* (as the already approved Spinraza). They demonstrated high efficacy of this PPMO after its systemic administration through facial vein at P0 in severe SMA mice model, both in the CNS and peripherally. These promising results make Pip6a-MO a promising starting point to develop a CPP-MO-based therapy for SMA [58].

Another CPP used for SMA is ApoE (141-150), a fragment of 10 amino acid (LRKLRKRLLR) belonging to the Apoliprotein E. In particular, it was

demonstrated an increased amount of *SMN2* transcript after treatment in fibroblasts, suggesting a better uptake of the MO mediated by the CPP conjugation [59]. Shabanpoor et al., investigated the efficacy of a branched derivative of ApoE (Br-ApoE) conjugated to PMO in *in vivo* SMA mouse model: the treatment resulted in an increased amount of functional SMN protein in the CNS, increased survival, weight, and muscle strength [60].

This work in mainly focused on two CPPs: the first, r6, is made up by six arginine with a D enantiomeric configuration, assuring a high internalization efficiency due to the lengths of its peptide backbone and stretch of arginine residues [61]; the second (RXRRBR)2XB (named RXR) has been tested for DMD and administered by intravenous and intramuscular injection, producing strong dystrophin expression in 100% of fibres in all skeletal muscles examined [62].

# 2. AIM OF THE THESIS

The causative gene of SMA is a mutation in *SMN1*, that causes the depletion of SMN protein. The paralogous *SMN2* has a different splicing pattern that leads to the production of only 10% of the functional protein. The first therapy approved, Nusinersen, is based on antisense oligonucleotides (ASO) that target *SMN2* splicing site leading to the retention of exon 7 and to the production of the full length functional SMN. However, these treatments have some concerns that remain unresolved:

- Narrow therapeutic window, usually limited to the presymptomatic phases;
- Invasive administration through repetitive intrathecal injections.

The principal aim of the thesis is to overcome these issues, in particular to develop a treatment that could be administered systemically in a less-invasive way to symptomatic patients and milder SMA cases. To do this, the thesis is organised in the following steps:

-Conjugating our already validated MO to four different CPPs (Tat, R6, r6, RXR) to evaluate biodistribution and effects on SMN expression in heterozygous mice at postanatal day 1 (P1);

-Analysing the results of a systemic less-invasive administration of the treatments in symptomatic SMA mice, assessing SMN level in CNS and in peripheral organs; amelioration of the neuropathological phenotype focusing on neuromuscular junctions' innervation, motor neuron count, gliosis and fibers size, motor behaviour and survival, toxic effects, MO biodistribution, and *Igf* levels.

Our results demonstrated that the conjugation of MO to CPPs is a promising and safe approach to ameliorate the biodistribution and the efficacy of the ASO-based treatment, suggesting a possible development of a non-invasive treatment also for symptomatic and milder SMA patients.

# 3. MATERIAL AND METHODS

## 3.1. Morpholino Oligomers conjugation

The 25-nt PMO sequence used in this work is the following: GTAAGATTCACTTTCATAATGCTGG. It was designed and manufactured by Gene Tools to target the 15-nt negative intronic splicing silencer N1 (ISS-N1) region in the SMN2 gene [47]. MO10-34 has been covalently linked to cell-penetrating peptides (CPPs) by our external collaborator Dr. Hong Moulton (University of Oregon). CPPs were attached to PMO 5' end through a non-cleavable maleimide bond [63] resulting in different P-PMOs [64]. Four different arginine-rich CPPs were used, synthetized by Peptide 2.0 Inc.:

- HIV Tat peptide (sequence: YGRKKRRQRRRQ);
- R6 peptide (sequence: RRRRRR, L enantiomeric configuration);
- r6 peptide (sequence: RRRRRR, D enantiomeric configuration);
- RXR peptide (sequence: (RXRRBR)2XB).

For control groups, we used the vivo-MO scramble designed on our 10-34 sequence.

Lyophilized compounds were dissolved in deionized sterile water with a concentration of 5 nMoles/gr.

## 3.2. Animal Model

All transgenic animals were purchased from The Jackson Laboratory. All animal experiments were approved by the University of Milan and Italian Ministry of Health review boards according to the institutional guidelines that are in compliance with national (D.I. no. 116, G.U. suppl. 40, February 18, 1992, Circolare no. 8, G.U., 14 Luglio 1994), approved protocol 1007-2016-PR.

We used JAX stock #005025: FVB.Cg-Grm7$^{Tg(SMN2)89Ahmb}$ Smn1$^{tm1Msd}$ Tg(SMN2*delta7)4299Ahmb/J, a mouse model of type I/II SMA, called also SMAΔ7 mouse. This strain has a FVB/N genetic background and is a triple mutant mice harbouring:

- *Smn1* targeted mutation
- two transgenes:
    - Tg(SMN2)89Ahmb, a human *SMN2* gene full length under the control of human *SMN2* promoter
    - Tg(SMN2*delta7)4299Ahmn, a human *SMN2* cDNA lacking the exon 7 under the control of human *SMN2* promoter [65].

Heterozygous animal for *Smn1* (*Smn*$^{+/-}$; *SMN2*$^{+/+}$; *SMN*Δ*7*$^{+/+}$) were bred together to obtain mice that are homozygous knockout for *Smn1* allele (*Smn*-/-) and homozygous for the other two transgenic alleles (*SMN2*$^{+/+}$; *SMN*Δ*7*$^{+/+}$). These mice (*Smn*$^{-/-}$; *SMN2*$^{+/+}$; *SMN*Δ*7*$^{+/+}$) display SMA phenotype and are named SMA mice.

3.2.1. Genotyping

To distinguish the homozygous affected animals we performed a quick DNA extraction protocol from tail biopsy based on hot sodium hydroxide and Tris (HotSHOT) [66]. Genotyping was performed by a separated touchdown PCR protocol, which increase the specificity of the reaction. The primers (Sigma) used are listed below:

| **Primer** | **Sequence 5'→3'** | **Target** |
|---|---|---|
| SMA_08 (oIMR7208) | CTC CGG GAT ATT GGG ATT G | Mutant Forward |
| SMA_10 (oIMR7210) | GGT AAC GCC AGG GTT TTC C | Mutant Reverse |

| | | |
|---|---|---|
| SMA_39 (oIMR3439) | TTT TCT CCC TCT TCA GAG TGA T | Wild type Forward |
| SMA_40 (oIMR3440) | CTG TTT CAA GGG AGT TGT GGC | Wild type Reverse |

The two PCR reaction mixes are the following:

**Reaction A**

| **Reaction component** | **Final concentration** |
|---|---|
| ddH2O | Up to final volume (50 µl) |
| 10X PRC Buffer, Minus Mg (Invitrogen) | 1.3X |
| MgCl2 (Invitrogen) | 2.6 mM |
| dNTP Mix (Invitrogen) | 0.26 mM |
| Primer 7208 | 0.5 mM |
| Primer 7210 | 0.5 mM |
| Platinum Taq DNA polymerase (Invitrogen) | 0.03 U/ul |
| DNA | 50-200 ng |

**Reaction B**

| **Reaction component** | **Final concentration** |
|---|---|
| ddH2O | Up to final volume (50 µl) |
| 10X PRC Buffer, Minus Mg (Invitrogen) | 1.3X |
| MgCl2 (Invitrogen) | 2.6 mM |
| dNTP Mix (Invitrogen) | 0.26 mM |

| | |
|---|---|
| Primer 3439 | 0.5 uM |
| Primer 3440 | 0.5 uM |
| Platinum Taq DNA polymerase (Invitrogen) | 0.03 U/ul |
| DNA | 50-200 ng |

The PCR amplification products were separated by gel electrophoresis on a 1.5% agarose gel with the use of a loading dye of 50% glycerol in Tris-acetate-EDTA (TAE), additioned with bromophenol blue. SMA mice are the ones that result positive for *SMN2* transgene (reaction A) and negative for the internal positive control *Smn1* (reaction B).

### 3.3. CPPs-Morpholino treatments

#### 3.3.1. Intravenous (IV) administration

A systemic intravenous (IV) injection through facial vein was performed in P1 heterozygous SMA mice (n=6 per treatment). We visualized the partial vein near the ear bud and the needle was inserted with a 45° angle as previously described [67], and the compound was administered. We tested both the naked MO 10-34 and the 4 different PPMOs at a dosage of 12 nmoles/g [47].

#### 3.3.2. Intracerebroventricular (ICV) injection

The ICV injection was performed as previously described [47]: mice (n=6/group) were hand-mounted over a back-light to visualize the intersection of the coronal and sagittal cranial sutures (bregma). A fine-drawn capillary needle with injection assembly was then inserted 1 mm lateral and 1 mm posterior to bregma and then tunnelled approximately 1 mm deep from the skin edge, corresponding to the ipsilateral lateral ventricle.

### 3.3.3. Intraperitoneal (IP) administration

In SMA mice a systemic administration through intraperitoneal (IP) injection of 12 nMoles/gr of treatment was performed at P5 (symptomatic phase) (n=4 per treatment for western blot analysis, n=at least 6 per treatment for survival and phenotypical analysis, n=2 per treatment for toxicity analyses, n=at least 3 per treatment for histopathological analyses, n=3 per treatment for ELISA, n=at least 4 per treatment for qPCR). Other doses (6 and 9 nMoles/gr) were administered by IP injection (n=4 for western blot). The injection was made perpendicularly into the intraperitoneal lower left quadrant for no more than 0.5 cm of the needle, as previously described [68]. The compounds were tested again at 12 nmoles/g. For this kind of administration, we only used naked MO, r6-MO and RXR-MO. Another symptomatic treatment at P7 was performed (n=8 per treatment for survival and phenotypical analysis).

### 3.4. Western Blot

For western blot (WB) analysis, 20 mg of organs of interest (brain, spinal cord, muscles, liver and heart) were collected, directly frozen in nitrogen and stored at -80°C. Then were added to a lysis buffer solution (4x NuPAGE LDS Sample Buffer) composed of Tris-HCl 0.5 M, glycerol 10%, 2-β-mercaptoethanlol 3%, bromophenol blue 0.003%, SDS 2.5% Tris base (141 mM), Tris HCl (106 mM), LDS (2%), EDTA (0.51 mM), SERVA Blue G-250 (0.22 mM), phenol red (0.175 mM), pH 8.5 and a set of proteases inhibitors at pH=6.8. Each sample was sonicated twice for 10 seconds at ~40w, then boiled for 4 minutes and centrifuged for 13 minutes at 13200 rpm. After extraction, protein concentration was evaluated through Pierce Comassie Plus Protein Assay Lowry assay. Next, 35 µg were collected from each mixture with DTT (reducing agent) and charged on a 4-12% gradient polyacrylamide gel (Invitrogen NuPAGE Bis-Tris) with sodium dodecyl

sulfate (SDS-PAGE). Then, they were transferred on a nitrocellulose membrane, saturated with Intercept Blocking Buffer PBS (LI-COR) 1% BSA (), 10% horse serum, 0.075% Tween 20 at 0.075% in TBS solution (20 mM Tris-HCl, 0.5 M NaCl 0.5 M) for 1one hour at RT. Membrane was then incubated ON at 4°C in a blocking solution containing primary antibody anti-SMN (1:800, Millipore)– 1 hour with α-actin 1:2.000 (Sigma) as control protein. The following day, membrane was washed three five times with PBS-T solution (20 mM Tris-HCl, 0.5 M NaCl 0.5 M, 0.05% Tween 20 0.05% 0,08%) and incubated at RT for one 1 hour with secondary anti-body (anti-mouse IR-DYE 800 CW 1:20000) in blocking solution. Bands were visualized through LI-COR Biosciences, Odissey FC while densitometric analysis of fluorescence signal was performed using the software Image Studio ™ (LI-COR Biosciences).

### 3.5. Real Time PCR

RNA was extracted with ReliaPrep RNA Miniprep System (Promega) according to manufacturer instructions. Cells were washed twice with PBS before to be lysed directly in the plate with the lysis buffer from the kit and stored at -80°C until extraction. RNA quantity and quality were assessed by spectrophotometric analysis with NanoDrop One (ThermoFisher) and 260/280 nm and 260/230 nm absorbance ratio evaluation.

Retrotranscription of extracted RNA was performed with the Ready-To-Go You-Prime First-Strand Beads (GE Healthcare) using from 100 ng to 5 µg of RNA producing cDNA stored at -20°C for gene expression analysis. Gene expression was quantified by real-time qPCR on 7500 Real-Time PCR System (Applied Biosystems) with TaqMan molecular probes or standard primer-based SYBR green detection with and their respective commercially available TaqMan™ Universal PCR Master Mix (Applied Biosystems) or

Power SYBR™ Green PCR Master Mix (Applied Biosystems). Cycle thresholds were normalized on reference gene and fold change were calculated by ΔΔCt method.

### 3.6. Enzyme-Linked Immunosorbent Assay (ELISA)

To quantify MO delivered to different organs by the conjugation with either the RXR or r6 peptide, independently from SMN levels, we performed an ELISA method based on a previously described protocol [69]. Naked and r6-MO mice (n=3/group) were sacrificed 48 hours after IP treatment (P7), and the brain (n=5/group), spinal cord (n=3/group), liver (n=3/group), quadriceps muscle (n=5/group), and heart (n=3/group) were harvested. After homogenization and trypsin digestion, tissues were eluted and tested in triplicate on a Neutravidin-coated plate at room temperature overnight and hybridized with a specific probe complementary to our MO sequence (Eurofins). After washing, the plate was incubated with 5-U/well Micrococcal Nuclease, the optimal enzyme concentration determined for our probe. After incubation with Antidigoxigenin AP-coniugated antibody and subsequently with the Attophos substrate, the plate reading was performed with Varioskan™ LUX multimode microplate reader (Thermo Fisher Scientific, USA). Four control wells in duplicate were added in each plate to determine the background signal.

### 3.7. Phenotypical tests

Each day, observers monitored all injected animals (wild-type (wt) n=6, scr-MO n=10, naked MO n=12, r6-MO, or RXR-MO n=8/group), as well as breeding pairs, for morbidity, mortality, and weight. All treated animals underwent phenotypic tests and weight measures twice a week up to P14, then weight was measured once a week.

### 3.7.1. Hind-limb suspension test

Hind-limb suspension test evaluates the positioning of the legs and tail. Mice were suspended by their hind limbs from the lip of a standard 50-mL plastic centrifuge tube. The posture was scored from 0 to 4 as previously described [65].

### 3.7.2. Righting reflex

Righting reflex assay was performed turning each pup onto its back and evaluating its ability to stably place all four paws on the ground [65].

### 3.7.3. Rotarod

The Rotarod test (Rota-Rod 7650; Ugo Basile) was performed from P45 once a month, using a 4-phase profile as previously described [47].

## 3.8. Histological analyses

Mice (n=3) of each group treated at P5 were sacrificed at different day:naked-MO and scr-MO at P10, r6 and RXR-MO at P10 and P30.

### 3.8.1. Muscle stainings

Intercostal and quadriceps muscles were collected, directly frozen on dry ice and stored at -80°. Samples were put at least one night at -80°C before being sectioned by cryostat (Leica) with a thickness of 20 µm, mounted on glass slides, and stored at -80°C.

NMJs analyses

For Neuro Muscular Junctions (NMJs) analyses muscle sections were washed once with PBS 1X and permeabilized for 5 minutes in 0,25% Triton-X-100 in PBS. Then, they were blocked with a blocking solution (10% mouse serum in 0,25% Triton-X-100-PBS) for 1 hour at RT and incubated ON at 4°C with the primary antibody against NF-M (Millipore, rabbit, 1:250 in blocking

solution). The next day the slides were washed three times with PBS 1X to remove the residues of the primary antibody and then incubated for 1.30 hour at RT with the secondary specific antibody (Alexa 488 anti-rabbit, Invitrogen, 1:1000 in PBS 1X). After 3 washing in PBS 1X to remove the secondary antibody, the samples were incubated for 3.30 hours at RT with alpha-bungarotoxins conjugated with Alexa 555 (Invitrogen, 1:200 in PBS 1X). After that, the slides were washed repeatedly again with PBS 1X and incubated for 5 minutes at RT with DAPI (1:1000 in PBS 1X). Finally, after 3 washing in PBS 1X the coverslips were mounted with the use of Fluor Save Reagent (Calbiochem). Images of the stained intercostal muscles were acquired with a confocal microscope LEICA SP8. We counted the total number of NMJs and the percentage that was innervated by the axons, when the two signals merged. As already described [47] we consider at least 100 NMJs from each muscle. The same images were analysed with ImageJ software to measure endplate areas: areas marked by α-bungarotoxin were encircled/trimmed with a specific tool and measured in at least 100 NMJs [70].

Quadriceps muscle fibers and cross-sectional area

We performed a hematoxylin/eosin staining on intercostal muscle slices of CPPs-MO-treated, naked-MO-treated and scramble mice: slides were incubated 50 seconds in Hematoxylin reagent and washed in water. Then slides were stained in eosin reagent for 20 seconds, rinsed, incubated in EtOH for 5 minutes and washed twice in EtOH. Finally, slides were rinsed three times in xylene and mounted with cover slides. To measure cross sectional areas of muscle fibers, pictures of hematoxylin/eosin staining were acquired by optical microscope and fibers perimeters were encircled/trimmed using

ImageJ. Areas were measured as previously described [71] for at least 100 fibers.

### 3.8.2. Spinal cord

Spinal cords were harvested and were fixed in a 4% paraformaldehyde solution (PFA) for 24 hours at 4°C. The next day they were washed with a phosphate buffer saline (PBS) 1X solution and immersed in 30% sucrose solution in PBS overnight (ON). the lumbar part of the spinal cords, free from the backbone part, was cut and divided in L1-L2 and L3-L5, immersed in Optimal Cutting Temperature compound OCT (Tissue Tek), frozen on dry ice and stored at -80°C for at least one night before being sectioned by cryostat (Leica) with a thickness of 20 μm, mounted on glass slides, and stored at -80°C.

Motor Neuron staining and count

Spinal cord serial sections were washed once with PBS 1X and blocked in a blocking solution (10% Normal Donkey Serum in 0,3% Triton-X-100-PBS) for 1 hour at RT. Then the slides were incubated ON at 4°C with primary antibody (ChAT, Millipore, 1:250 in blocking solution). The next day the samples were washed three times with PBS 1X and incubated for 1.30 hours at RT with the specific secondary biotinylated antibody (biotinylated anti-goat antibody, Vector Laboratories, 1:400 in PBS 1X). After that, the slides were washed three times with PBS 1X to remove the remaining secondary antibody and then they were incubated for 1 hour at RT with Streptavidin Cy3 (Sigma Aldrich, 1:400 in PBS 1X). Then the samples were washed three times with PBS 1X and incubated for 5 minutes at RT with DAPI (1:1000, Invitrogen in PBS 1X). Finally, after three washing in PBS 1X, and with the use of Fluor Save Reagent (Calbiochem) the coverslips were mounted on the slides. Images were processed at an optical microscope, and cells that

exhibited fluorescent MN specific ChAT signal in the ventral horn were counted. We analysed serial sections (n=30) for each zone (L1-L2 and L3-L5) at 20X magnification to determine the mean number of MNs per spinal cord region and for the total spinal cord (L1-L5) MN number for each animal.

Gliosis

To assess the presence of gliosis in spinal cord mice (n= 4/group), we blocked spinal cord slices in PBS 1X with 10% NGS and 0,3% Triton X-100 for 1h at room temperature. GFAP primary antibody (1:500, Abcam) was added overnight at 4°C, then the slides were incubated with Alexa 488 secondary antibody (1:1000, Life Technologies) for 1.5 hours at RT. Once the cover slides were mounted, to perform a semi-quantitative analysis, we acquired from 4 to 6 images of spinal cords half-slices for each treatment at 20x with a confocal microscope LEICA SP8, in order to count at least n=100 nuclei, and divided the number of nuclei surrounded by more than 50% of their perimeter by GFAP by the total number of cells [72].

### 3.9. Toxicity evaluation

To investigate possible toxic effects of our treatment we collect the blood from mice (n=2) treated with r6-MO, RXR-MO, and untreated, during the dissection procedure. The blood was left 30 minutes at RT and then centrifuged for 10 minutes at 3500 rcf. The resulting supernatant, the serum, was transferred in new eppendorf and stored at -20°C. The serum samples were then analysed by Charles River Laboratories for a list of toxicity biomarkers (Glucose; Creatinine; Urea; Total cholesterol; Total protein; Total bilirubin; Alkaline phosphatase (ALP); Alanine transaminase (ALT); Creatine kinase (CK); Lactate dehydrogenase (LDH)).

### 3.10. Statistical analysis

All statistical analyses were performed using Prism software. Data were expressed as mean ± standard error of the mean (SEM). All data were analysed using one-way ANOVA for multi-comparison analyses followed by Tuckey post-hoc tests and the Student t-test to compare each CPP-MO treatment with naked MO. NMJ innervation and righting test were analysed with contingency test following by Fisher test. Kaplan-Meier survival analysis and log-rank test were used for survival comparisons. Values were considered significant when *P* value was less than 0.05.

# 4. RESULTS

## 4.1. SMN level in the CNS increase after CPPs-MO treatment

### 4.1.1. Selection of the best peptides

We conjugated our validated MO sequence targeting the ISS-N1 region within SMN2 (HSMN2Ex7D 10–34) [47] with one of four different CPPs (Tat, R6, r6, and RXR). To verify the ability of each CPP to deliver the MO to the CNS and increase the amount of SMN protein, and to select the most efficient conjugate for further experiments, we performed an intracerebroventricular (ICV) (Fig. 7A, C and E) or intravenous (IV) (Fig. 7B, D and F) injection with the four different CPP-MOs at a concentration of 12 nmoles/g body weight in heterozygous SMAΔ7 mice at P1. Western Blot (WB) results confirmed the superiority of CPP-conjugated MOs in significantly increasing the level of SMN protein in both brain (Fig. 7 C and D) and spinal cord (Fig.8E-F, $P < 0.001$ in brain ICV; $P < 0.05$ in brain IV and spinal cord ICV; $P < 0.01$ in spinal cord IV). The r6 and RXR peptides were the most effective in rescuing SMN if compared to naked MO ($P < 0.05$). Therefore, these peptides were selected for the subsequent experiments in symptomatic SMA mice.

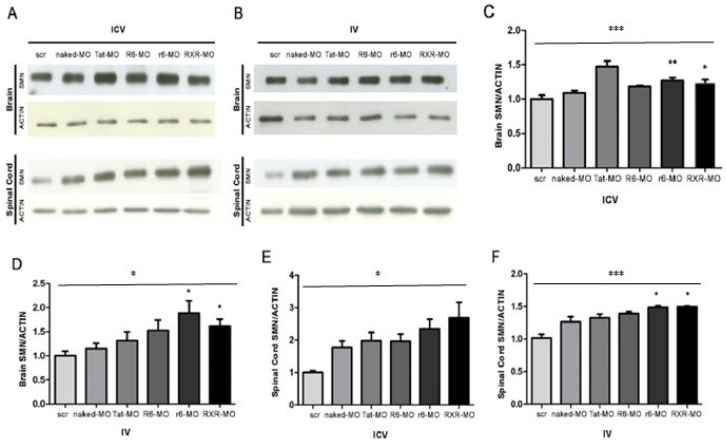

**Fig. 7. r6 and RXR peptides are the most efficient in carrying MO to CNS**

Representative image of WB for SMN and actin (**A**) and densitometric analysis of brain (**B**, **D**) and spinal cord (**C, E**) of heterozygous SMA mice treated ICV (**B, C**) and IV (**D, E**) at P1 with 12 nmoles/gr dose of naked MO, Tat-MO, R6-MO, r6-MO, RXR-MO, and sacrificed at P7. Scr-animals were used as controls. Relative amounts of SMN were normalized on the actin levels as mean value (n=6 mice/group). Statistical significance was determined using ANOVA (*$P < 0.05$, ***$P < 0.001$) and Student's *t* test for r6- and RXR- vs naked MO ($P < 0.05$).

### 4.1.2. Symptomatic treatment by systemic injection

We tested the selected RXR-MO and r6-MO conjugates in SMAΔ7 mice at P5, which corresponds to a symptomatic phase of SMA. We injected the scrambled control (scr-MO), the naked MO, and the r6/RXR-conjugated MO at the concentration of 12 nmoles/g by systemic intraperitoneal (IP) injection. Mice (n=4/group) were sacrificed 48 hours after treatment. WB analysis of brain and spinal cord revealed a striking increase in SMN protein in mice treated with the CPP-MO conjugates (Fig. 8A). Statistically significant results were obtained in the brains ($P < 0.05$, Fig. 8B) and in the spinal cord ($P < 0.01$, Fig. 8C) of mice treated with conjugates. These data demonstrated that systemically administered select CPPs can deliver MO to the CNS, even in a symptomatic phase, when the blood-brain barrier (BBB) is completely closed [40,73]. Further WB analyses were performed on heart, liver, and kidney (Fig. 8D), and confirmed the significant increase in SMN levels in the livers and hearts ($P < 0.01$, Fig. 9E), as well as in the kidneys ($P < 0.05$, Fig. 8E) of CPP-treated mice.

We also tested lower doses of conjugates by injecting IP 9 nmoles/g (n=4/group), but WB analysis showed no difference in SMN levels in the CNS after those treatments (Fig. 9A, B).

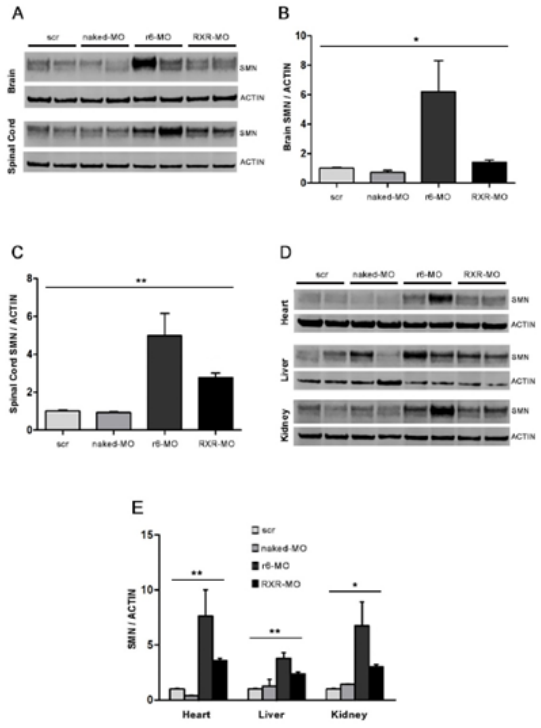


**Fig. 8. Treatment with CPP-MOs by IP injection at P5 increases SMN levels in SMA mice**

Representative image of WBs for SMN and actin (**A**, **D**) and their densitometric analysis (**B**, **C**, **E**) performed on protein extracted from brain (**B**), spinal cord (**C**), and heart, liver, and kidney (**E**) from SMA mice treated IP at P5 with 12 nmoles/g of naked MO, r6-MO, or RXR-MO, and sacrificed at P7. Scr-MO animals were used as controls (4 mice/group). Relative amounts of SMN were normalized to actin levels as mean ± SEM. Statistical significance was determined using one-way ANOVA (*$P < 0.05$, **$P < 0.01$) and Student's $t$ test comparing CPP-MOs vs naked MO ($P < 0.05$).

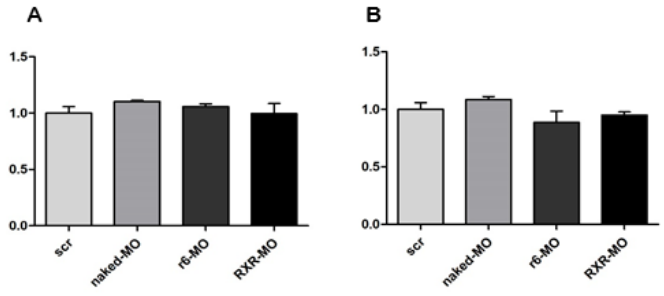


**Fig. 9. Treatment with 9 nMoles/gr CPP-MOs by IP injection at P5 does not change SMN levels in SMA mice**

Stacked bar plot of densitometric analysis of protein extracted from brain (**A**), spinal cord (**B**), from SMA mice treated IP at P5 with 9 nmoles/g of naked MO, r6-MO, or RXR-MO, and sacrificed at P7. Scr-MO animals were used as controls (4 mice/group). Relative amounts of SMN were normalized to actin levels as mean ± SEM.

## 4.2. MO biodistribution

To collect data about the real biodistribution of naked MO and CPP-MOs, independent from the SMN level, we performed an ELISA assay designed to specifically detect our MO sequence. We assessed MO levels in brain, spinal cord, heart, quadriceps, and liver of symptomatic SMA mice treated at P5 with naked MO and r6-MO, which is the best peptide according to WB, by IP injection (Fig. 10). Conjugation with r6 allowed MO to reach all of these organs, with an average MO detection of 7298 pM in spinal cord, 5271 pM in heart, 85780 pM in liver, and 6061 pM in muscle. Our data showed a significantly higher amount of MO delivered by the r6 peptide compared to the naked MO in liver ($P < 0.05$), spinal cord ($P < 0.05$), muscle ($P < 0.05$) and heart ($P < 0.001$). In brain samples, we found only a trend towards increase (data not shown), but basal values were always low and not reliable, suggesting possible technical problems related to this specific tissue.

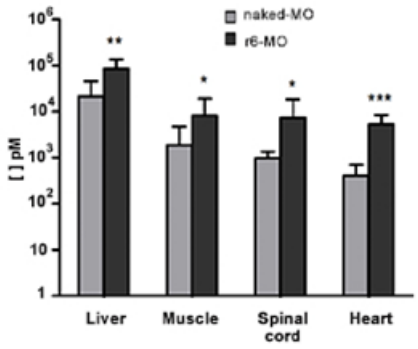


**Fig. 10. Treatment with CPP-MOs by IP injection at P5 delivers MO to multiple organs**
Stacked bar plot of ELISA assay results for MO presence in brain, spinal cord, liver, heart, and muscle from SMA mice treated IP at P5 with 12 nmoles/g of naked MO or r6-MO, and sacrificed at P7. Scr-MO animals were used as controls. Statistical significance was determined using Student's *t* test comparing CPP-MO vs naked MO (**P* < 0.05, ***P* < 0.01, ****P* < 0.001, at least 3 mice/group).

## 4.3. Phenotype rescue

### 4.3.1. CPPs-MO treatment in a symptomatic phase increases survival

To evaluate the effects of CPP-conjugated MOs on the disease phenotype, we treated symptomatic SMAΔ7 mice at P5 with 12 nmoles/g of r6-MO or RXR-MO (n=8/group), compared with naked MO mice (n=10). Mice injected with the scr-MO (n=12) were used as controls. Treated mice were monitored daily with regard to the phenotypic disease hallmarks and survival, until the end stage. Mice treated with the scramble (scr) or naked MO presented cases of paralysis and death in the first 2 weeks, with a median lifespan of 12 days for the scr- and 17 days for the naked MO symptomatic mice (Fig.11A). Treatment with either CPP-conjugated MO significantly improved the survival and functional condition of symptomatic SMA mice compared with scr-MO- and naked MO mice. Kaplan-Meier curves showed an overall

statistically significant increase in survival with CPP-MOs ($P < 0.001$, $\chi 2 = 45.39$ Fig.11A). Strikingly, when compared with the naked MO, CPP-MOs improved median survival (17 days for the naked MO) to 41.4 days for r6-MO ($P < 0.001$, $\chi 2 = 16.91$) and 23 days for RXR-MO ($P < 0.01$, $\chi 2 = 9.157$) (Fig.11A).

In order to further investigate the therapeutic window of CPP-MO treatment, we also treated SMA mice at P7 and P10 by IP injection. We observed that survival after P7 treatment (n=8 per treatment) did not improve compared with naked MO and scr-MO treated mice (average survival: 13.1 days for r6-MO and 15.2 days for RXR-MO, Fig.11B). Moreover, we treated SMA mice at P7 by ICV injection to be sure the entire dose of treatment could reach the brain, but observed no remarkable increase in lifespan, suggesting that treatment at P7 is too late to obtain any rescue of the disease.

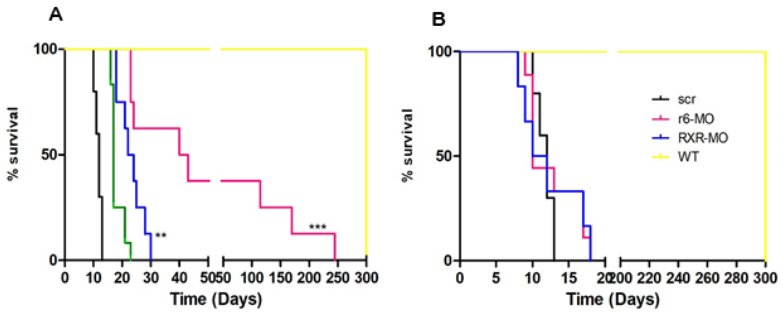


**Fig. 11. Treatment with CPP-MOs by IP injection at P5 extends the survival of SMA mice, while injection at P7 has no effect**

**A:** Kaplan-Meier survival curve of wild type and SMA mice treated IP at P5 with scr-MO (n=10), naked MO (n=12), r6-MO, or RXR-MO (n=8/group); CPP-MOs significantly enhanced survival (***$P < 0.001$, $\chi 2 = 14.59$, **$P < 0.01$, $\chi 2 = 9.157$). **B:** Kaplan-Meier survival curve of wild type and SMA mice treated IP at P7 with scr-MO, naked MO, r6-MO, or RXR-MO (n=8/group).

### 4.3.1. CPPs-MO treatment in a symptomatic phase ameliorates motor functions

Scr-MO and naked MO mice presented muscle weakness starting from the injection day (P5). Indeed, when laid on their backs, they were not able to turn and stand on four paws in the righting test (Fig.12A) and, when suspended by the tail, they were not able to extend their hind limbs during the tube test (Fig. 12B) and never reached the age (45 days) to perform the Rotarod test. CPP-MO-treated mice did not develop eye or ear necrosis after month 5, maintained good motor skills and autonomous movement and presented better performance compared with naked MO mice in the righting test at different time points (for r6-MO $P < 0.001$, all time points; for RXR-MO $P < 0.001$ at P10 and $P < 0.05$ at P13, Fig. 12B). The improvement related to the naked MO was also observed in the tube test at P10 ($P < 0.05$ for r6-MO) and at P13 ($P < 0.001$ for r6-MO, $P < 0.05$ for RXR-MO, Fig. 12B), and in the results of the Rotarod test (Fig. 12C), which was successfully completed by the majority of r6-MOs mice. Comparing the two CPP-MOs, r6-MO treated mice always performed better than RXR-MO ones, showing greater efficacy in rescuing the disease phenotype.

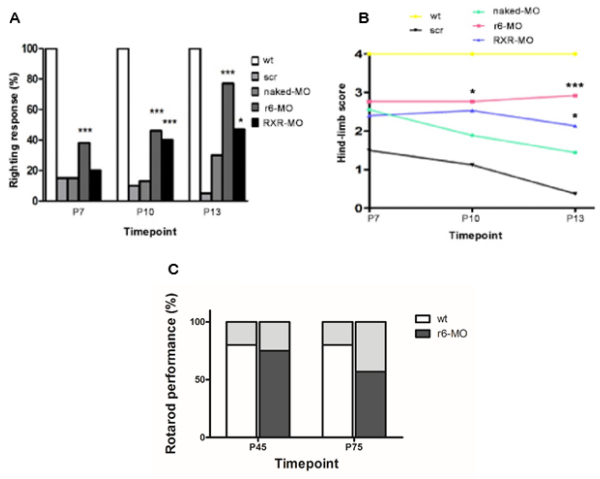


**Fig. 12. Treatment with CPP-MOs by IP injection at P5 extends the survival and ameliorates the phenotype of SMA mice**

**A:** Stacked bar plot of the percentage of positive righting reflex responses in wild type and SMA mice treated IP at P5 with naked MO, r6-MO, or RXR-MO at three different time points showing improvement with CCP-MO in comparison with naked MO treatment (scr-MO n=10, naked MO n=12, r6-MO, RXR-MO n=8, r6-MO: ***$P < 0.001$, all time points; RXR-MO: ***$P < 0.001$ at P10 and *$P < 0.05$ at P13, contingency and Fisher tests, CPP-MO vs naked MO). **B:** Mean tube-test hind-limb scores on a 0–4 scale. SMA mice were treated IP at P5 with scr-MO, naked MO, r6-MO, or RXR-MO at three different time points. Mice treated with CPP-MOs performed significantly better than mice treated with naked MO (scr-MO n=10, naked MO n=12, r6-MO, RXR-MO n=8, r6-MO: *$P < 0.05$ at P10 and ***$P < 0.001$ at P13, RXR-MO: *$P < 0.05$ at P13, Student's *t* test, CPP-MO vs naked MO). Values are presented as means ± SEM. **C:** Stacked bar plot of Rotarod performance test results of wild-type and SMA mice treated IP at P5 with r6-MO. No scr-MO, RXR-MO or naked MO mice were alive at the two time points tested. Results are indicated as the percentage of animals that completed the test. The records were performed at two different time points P45 and P75.

## 4.4. Histopathological hallmarks in muscle and spinal cord ameliorates after CPPs-MO treatment

### 4.4.1. NMJ innervation and endplate area in intercostal muscle

SMAΔ7 mice develop neuropathological features starting from P5. One of them is the degeneration of neuromuscular junctions (NMJs), whose denervation increases with the progression of the disease [74]. The disease is also characterized by marked and progressive MN degeneration [3]. To better understand the mechanisms underlying phenotypic rescue after CPP-MOs treatment, we analysed scr-MO, naked MO, r6-MO, and RXR-MO mice treated by IP injection at P5 and sacrificed at P10 or P30 (n=4/group). The pathological hallmarks were observed in all the untreated, scr-MO, and naked MO mice at P10. Analyses at P30 could not be performed in these animals since they died around P15. Interestingly, in CPP-treated mice, we observed a marked amelioration of NMJ denervation at P10 compared with naked MO, 5 days after treatment, which was significant for r6-MO ($P < 0.001$, Fig. 13A, B). The recovery of peripheral synapses in r6-MO mice reached 60% innervation, while it did not surpass 40% in scr-MO and naked MO mice (Fig. 13B). At P30, innervation remained good, at 72% in r6-MO and 50% in RXR-MO treated mice, again confirming the superiority of r6-MO treatment ($P < 0.05$ r6-MO versus RXR-MO, Fig. 13C,D). We also observed a significant increase in the endplate area of NMJs in CPP-MO mice at P15 ($P < 0.001$, Fig. 13 E) which was maintained at P30, in particular for r6-MO (Fig. 13 F).

### 4.4.2. Muscle fibers

SMA mice typically present muscle fibre atrophy and smaller skeletal muscle size, particularly in the intercostal muscles [27]. Our data showed that CPP-MO treatment had beneficial effects on these pathological markers in

quadriceps muscles (Fig. 14A) tested with haematoxylin/eosin staining, showing larger and better organised fibres, with cross-sectional areas quantified in quadriceps significantly higher in CPP-treated mice (Fig. 14B; $P < 0.001$).

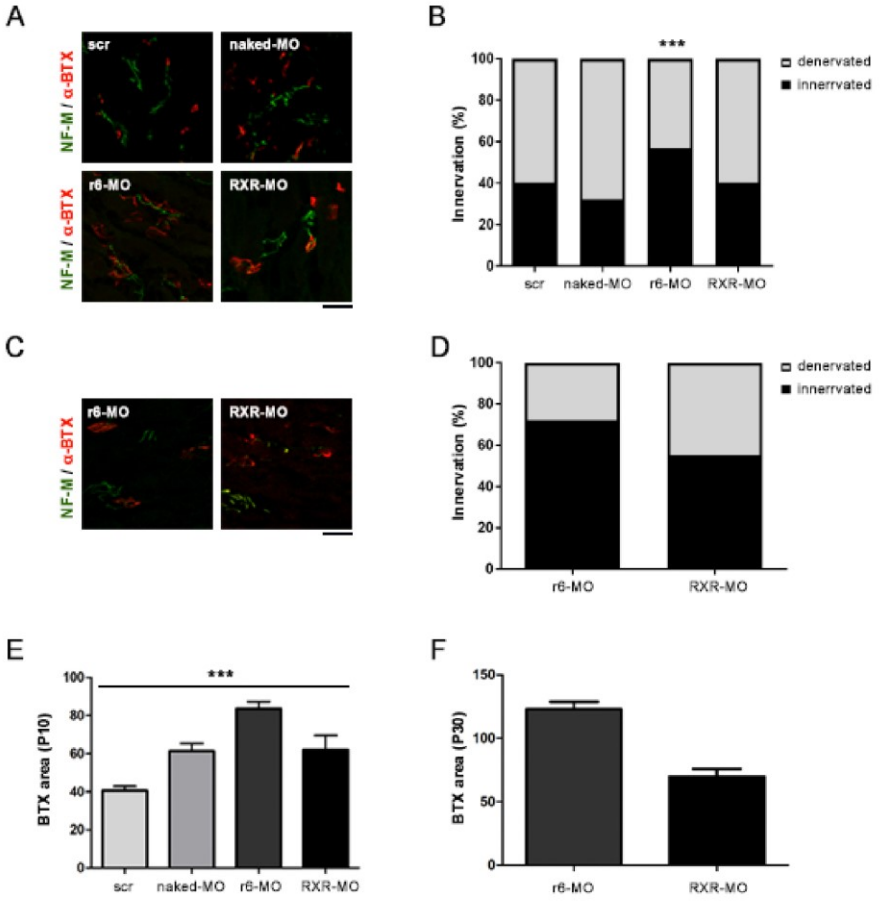


**Fig. 13. Treatment with CPP-MOs ameliorates intercostal muscle NMJ innervation in SMA mice**

**A**: Immunostaining of intercostal muscles from symptomatic SMA mice treated at P5 with scr-MO, naked MO, r6-MO, or RXR-MO sacrificed at P10 performed with NF-M antibody (green) and alpha-bungarotoxin antibody (red), magnification: 40X. **B**: Stacked bar plot of

the percentage of innervated (black) and denervated (light grey) NMJs in SMA mice at P10 (**P < 0.01, for r6-MO, n=100 NMJs, 4 mice/group, contingency and Fisher tests, CPP-MO vs naked MO). **C**: Representative image of NMJ staining of SMA mice treated with r6-MO or RXR-MO and sacrificed at P30. **D**: Stacked bar plot of the percentage of innervated (black) and denervated (light grey) NMJs in SMA mice at P30 (n=100 NMJs, 4 mice/group). **E, F**: Stacked bar plot of endplate area of NMJs in SMA mice at P10 (E) and P30 (F) (***P < 0.001, n=100 BTXs, n=4 mice/group, one-way ANOVA). Scale bar = 75 µm in **A** and **C**

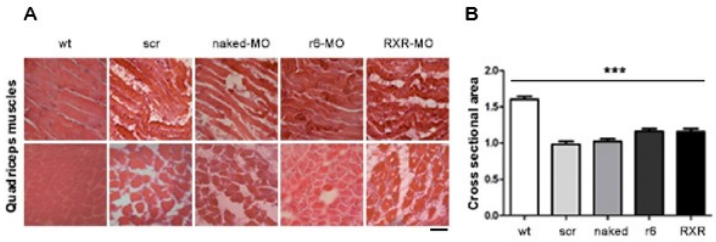


**Fig. 14. Treatment with CPP-MOs ameliorates muscle organization and size**

**A:** Representative image of haematoxylin/eosin staining of quadriceps muscles from SMA mice treated with scr-MO, naked MO, r6-MO, or RXR-MO and wild type mice, sacrificed at P10 (magnification: 40X) **B:** Stacked bar plot of muscle fibers cross sectional area in SMA mice at P10 (***$P$ < 0.001, n=100 fibers, n=4 mice/group, one-way ANOVA). Scale bar = 90 µm in **A**.

## 4.4.3. MNs number in spinal cord

Moreover, treatment with CPP-MOs increased the number of MNs. In spinal cords of mice sacrificed at P10, the number of MNs was significantly higher in CPP-treated mice ($P$ < 0.001; Fig. 15 A,B). The increasing trend was also confirmed in CPP-MO-treated mice sacrificed at P30 (Fig. 15 C,D).

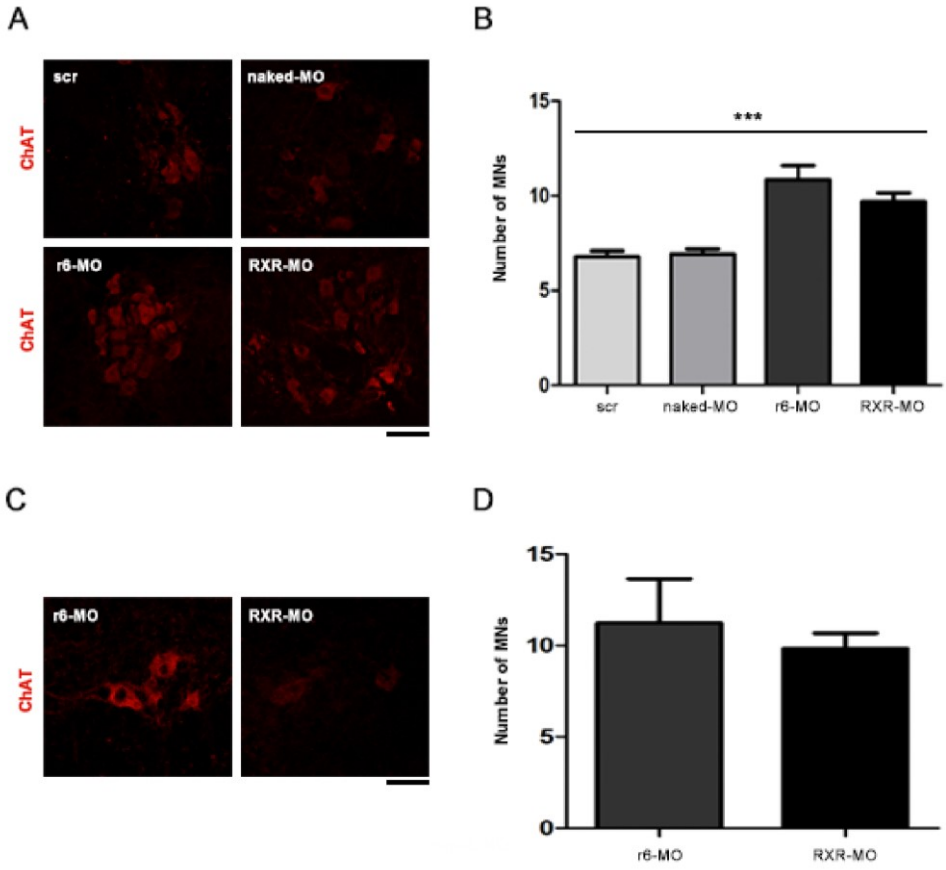


**Fig. 15. Treatment with CPP-MOs increases MN numbers in the spinal cords of SMA mice**

**A:** Representative image of MN staining of spinal cords from SMA mice sacrificed at P10. ChAT antibody staining (red) of spinal cord MNs from symptomatic SMA mice treated at P5 with scr, naked MO, r6-MO, or RXR-MO sacrificed at P10. **B:** Bar plot of MN numbers in SMA mice spinal cord at P10. Number of MNs was normalized to the scr-MO number as mean ± SEM. Statistical significance was determined using one-way ANOVA (***$P < 0.001$, n=60 slices, n=4/group). **C:** Representative image of MN staining in spinal cords from SMA mice treated with r6-MO or RXR-MO and sacrificed at P30. **D:** Bar plot of MN numbers in spinal cords from SMA mice at P30. Scale bar = 50 µm in **A** and **C**

### 4.4.4. Gliosis

Spinal gliosis is also known to be significantly high in SMA mice compared with wild type mice [3]. We investigated gliosis levels, identified by glial fibrillary acidic protein (GFAP) staining of spinal cord from wild type mice, scr-MO, and CPP-MOs treated SMA mice (Fig. 16A). The quantitative analyses showed higher levels of gliosis in scr-MO mice, while they significantly decreased in CPP-MOs mice ($P < 0.001$, Fig. 16B). All the experiments demonstrated the superiority of r6-MO compared to RXR-MO in ameliorating phenotype and delivering MO to CNS and peripheral organs.

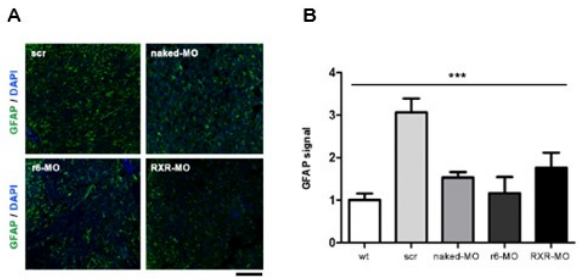


**Fig. 16. Treatment with CPP-MOs ameliorates gliosis in the spinal cords of SMA mice**
**A:** Representative image of GFAP staining of spinal cords from wild type mice and SMA mice treated with scr-MO, naked MO, r6-MO, or RXR-MO and sacrificed at P10. **B:** Bar plot of gliosis levels in spinal cords from SMA mice at P10. The number of nuclei surrounded by GFAP was normalized to the scr-MO number and reported as mean ± SEM. Statistical significance was determined using one-way ANOVA (***$P < 0.001$, n=100 nuclei, n=4/group. Scale bar = 90 μm in **A**

## 4.5. CPPs-MO treatment restores Igf1 and SMN expression in spinal cord and liver of treated mice

### 4.5.1. Igf1 and Igfals

The dysregulation of the *insulin-like growth factor 1 (Igf1*) gene axis and its rescue after systemic ASO administration were previously reported in an SMA mouse model [75]. We collected livers of treated SMA mice or wild type mice (n = 4/group) at P7 to see whether the IGF1 pathway was affected in our SMA model and modified by our treatments. Real-time qPCR results showed a significant decrease of both *Igf1* and *insulin-growth factor binding protein acid labile subunit* (*Igfals*) expression in scr-MO compared with wild type mice ($P < 0.001$ and $P < 0.01$ respectively, Fig. 17A, B). Treatment with r6-MO and RXR-MO tended to increase *Igf1* expression, with significantly higher levels in r6-MO-treated compared with naked MO mice ($P < 0.05$, Fig. 17C), while no significant variation was found in *Igfals* expression (Fig. 17D).

### 4.5.2. SMN expression

Notably, real-time qPCR assays performed on spinal cord samples of untreated and treated mice sacrificed at P7 disclosed that the CPP-MOs were able to significantly increase *SMN FL* expression levels ($P < 0.01$, Fig. 18A) as well as the *SMN FL/*Δ7 ratios ($P < 0.01$, Fig. 18B), indicating that the treatments improved the efficacy of exon7 inclusion.

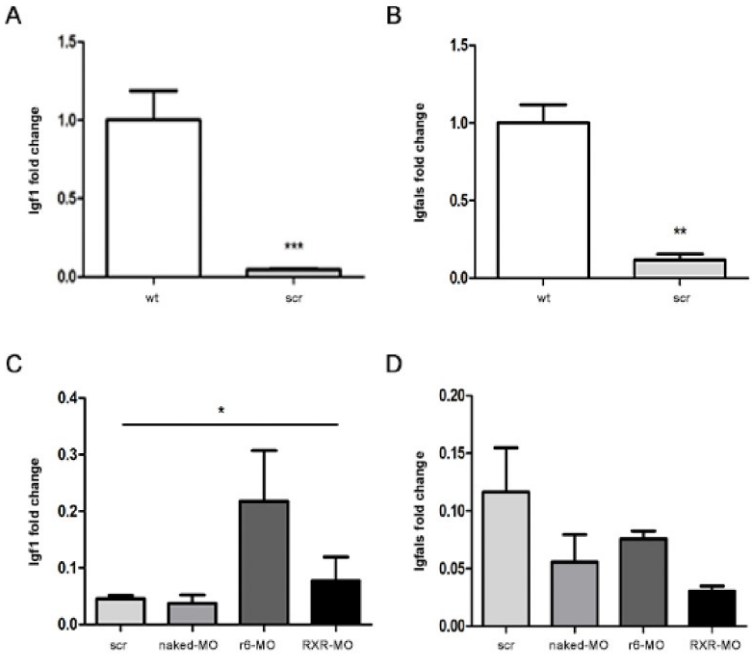


**Fig. 17. *Igf1* and *Igfals,* expressions are partially restored in CPP-MO treated mice**

**A**: Bar plot of liver *Igf1* expression in untreated wild type mice and scr-MO SMA mice sacrificed at P7 (***$P < 0.001$, Student's *t* test). **B**: Bar plot of liver *Igfals* expression in untreated wild type mice and scr-MO SMA mice sacrificed at P7 (**$P < 0.01$, Student's *t* test). **C**: Bar plot of liver *Igf1* expression in scr-MO, naked MO, r6-MO, and RXR-MO mice sacrificed at P7 (*$P < 0.05$, ANOVA). **D**: Bar plot of liver *Igfals* expression in scr-MO, naked MO, r6-MO, and RXR-MO mice sacrificed at P7. Data were normalized to the average levels of 18S RNA. Values are presented as means ± SEM, at least n=3/group.

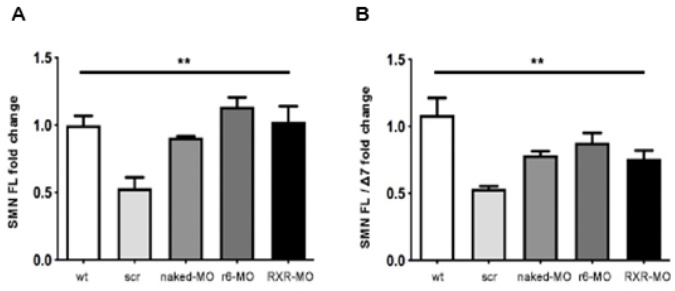

**Fig. 18. *SMN FL* and *SMN FL/ SMN Δ7* expressions are restored in CPP-MO treated mice**

**A:** Spinal cord *SMN FL* expression in wild type, scr-MO, naked MO, r6-MO and RXR-MO mice sacrificed at P7 (***P* < 0.01, ANOVA). **B:** Ratio of *SMN FL/ SMN Δ7* expression levels in spinal cord of wild type, scr-MO, naked MO, r6-MO and RXR-MO mice sacrificed at P7 (***P* < 0.01, ANOVA). Data were normalized to the average levels of *B-Actin*. Values are presented as means ± SEM, at least n=3/group.

## 4.6. CPPs-MO do not cause toxic effects in treated mice

To evaluate possible toxic effects caused by CPP-MO treatment, we collected serum from wild type mice and symptomatic mice IP treated with scr- or r6-MO or RXR-MO. Toxicological evaluation was performed on a standard set of biomarkers for liver and kidney toxicity, such as glucose, creatinine, urea, total cholesterol, total protein, total bilirubin, alkaline phosphatase, alanine transaminase, creatine kinase, and lactate dehydrogenase. All biomarker levels were comparable between the groups, suggesting that the treatments had no detectable toxic effects (Fig. 19).

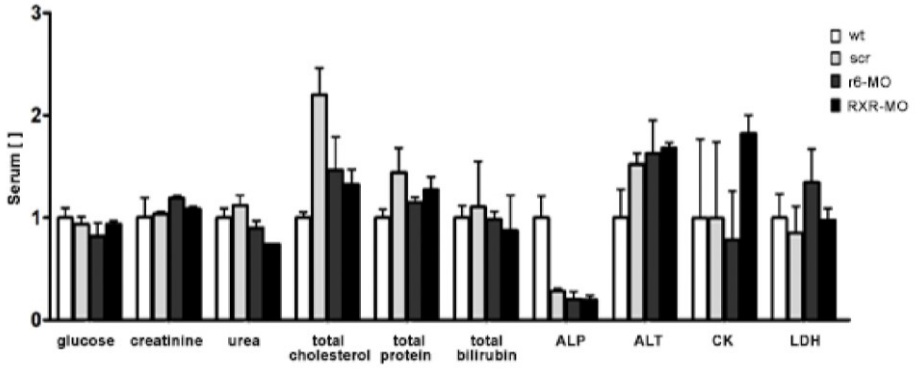


**Fig. 19. Treatment with CPP-MOs do not cause toxicity in SMA mice**

Stacked bar plot of toxicity markers analysed in wild type and SMA mice treated at P5 with 12 nmoles/g of r6-MO and RXR-MO (n=2/group. Measurement units for concentrations:

mg/dL for glucose, creatinine, urea, total cholesterol, total bilirubin; g/dL for total protein; U/L for alkaline phosphatase (ALP), alanine transaminase (ALT), creatine kinase (CK) and lactate dehydrogenase (LDH)).

# 4. DISCUSSION

SMA is a degenerative motor neuron disease, and the first genetic cause of infant mortality, caused by a mutation in *SMN1* gene [76]. Currently, there are three available treatments for SMA. The first, approved by FDA in 2016, is Nusinersen. It is an ASO-based therapy, administered by repeated intrathecal injections, which targets ISS-N1 region in intron 7 of *SMN2* inducing exon 7 retention and thus increasing the amount of the full length functional SMN protein [29]. This way of administration was selected to bypass directly the BBB, since ASOs are not able to pass across it; this requires trained staff, suitable facilities and can also be considered quite invasive, considering the majority of SMA patients are children. Another important concern about intrathecal delivery, is the impossibility to perform it in all the patients, like older SMA patients, who had spinal surgery to prevent scoliosis [77]. Moreover, Nusinersen targets specifically the CNS, while recent studies evidence that, for the complete rescue of the pathological phenotype, SMN restoration is necessary not only in the CNS, but also peripherally [78]. The major issue of Nusinersen and of all the available therapies is the narrow therapeutic window, which is optimal in the first 6 months of life in SMAI patients, which means in the early phase of the disease, with the best outcomes if administered in the pre-sintomatic phase [40]. In fact, for SMA symptomatic patients and milder SMA forms, currently there are no effective treatments available, suggesting the need of a functional therapy also for these patients.

To overcome these challenges a promising approach could be the use of Cell Penetrating Peptides (CPPs), conjugated to MO oligomers. CPPs allow the passage through biological membranes improving the biodistribution and the

kinetics of oligonucleotides. Since they can improve the crossing of the BBB to reach the CNS, they could be administered with a less invasive systemic route. Up until now, a MO-based therapy for DMD [79] has been already approved, and, specifically for SMA, CPPs-MO, conjugated to Pip6a, ApoE, Br-ApoE, have produced positive results in *in vivo* preclinical presymptomatic SMA models, demonstrating the feasibility of CPP-MO therapy also in SMA field [58,59]. Our study aims to demonstrate that CPP conjugation could be a promising approach to extend the narrow therapeutic window to the symptomatic phase of the disease, providing an improvement compared to the already approved therapies for SMA type I patients and making them suitable also for milder SMA types. To do that, we conjugated are validated MO sequence to four different CPPs: Tat -which is one of the most used in literature-, R6, r6 and RXR, and then injected the different compounds in pre-symptomatic mice to evaluate SMN rescue. Basing on the results and on toxic effects we excluded Tat and R6, and demonstrated that, even when delivered by IP injection at P5, the r6-MO and RXR-MO conjugates were able to cross the BBB and increase the distribution of MO better than naked MO, resulting in a higher level of SMN, acting increasing exon 7 inclusion. The high internalization efficiency of r6 conjugate likely depends on the lengths of its peptide backbone and stretch of arginine residues [61], while studies on RXR compound have shown a significant correlation between its splicing correction efficiency and its affinity for heparin and ability to destabilize model synthetic vesicles [80]. A peptide belonging to this particular class has shown promising results in delivering MO in DMD mice by IP injection, with a significantly superior effect on exon skipping and dystrophin restoration compared with the naked MO [81], while the same peptide ($[RXRRBR]_2XB$), administered by intravenous and intramuscular

injection, produced strong dystrophin expression in 100% of fibres in all skeletal muscles examined [62]. Recently, Sarepta Therapeutics initiated a Phase I/IIa clinical trial of a novel MO conjugated to a CPP, MO SRP-5051, targeting DMD patients amenable to exon 51 skipping [82] and further supporting the clinical translatability of our proposed CPP-MO injection for SMA.

We decided to perform our experiments using MO in a dose of 12 nmoles/g, corresponding to 102 μg/g of MO10-34, 130 μg/g of Tat-MO, 115 μg/g of R6 and r6 and 124 μg/g of RXR-MO, basing on preliminary experiments in which we tested three doses (6, 9 and 12 nmoles) and obtained good outcomes only with the highest one. Preliminary experiments in our work demonstrated that the CPPs-MO was able to cross better the BBB compared to the naked MO, when administered systemically by intravenous injection in presymptomatic mice, increasing the level of full length SMN in the CNS. This result supports the hypothesis that the amelioration of the biodistribution, mediated by MO chemistry and conjugation with CPPs, allows a systemic way of administration. This represents a promising result for clinic translation: many SMA patients have neuromuscular scoliosis or spinal instrumentation resulting in challenging intrathecal access. From these data, we selected the most efficacious compounds (r6-MO and RXR-MO) to be tested in symptomatic SMA mice.

We tested our CPPs-MO, r6-MO and RXR-MO, with a systemic low invasive IP injection in symptomatic SMA mice. It is the first time that a CPP-ASO is tested after P4 in a systemic way: Pip6a have been tested only in presymptomatic SMA mice to demonstrate SMN rescue, and in adult wild-type mice to assess the ability to pass the BBB [58]. Recently Kray et al tested MO effects in mice at P6, but together with the administration of the small

molecule RG7800; this combination demonstrated the amelioration of survival and phenotype in SMA mice [83]. The results we are presenting differ from the former because they show the efficacy of the treatment with CPPs-MO in rescuing SMN level both in the CNS and in peripheral organs, after systemic administration, during the symptomatic phase. Up until now, unconjugated MO or ASOs tested in symptomatic mice showed a significant decrease of therapeutic efficacy. Indeed, Porensky et al., treated SMA mice at P4 ICV (54 μg/g) or IV (50 μg/g), obtaining modest results in term of survival, and enlighting once again the necessity of early and targeted administration.

The fact that unconjugated MO could not provide the same results as conjugated MO after symptomatic injection, neither in our works nor in others, is probably due to the therapeutic window [40]. Strikingly, our results performed on symptomatic mice treated with CPPs-MO showed impressive survival rescue compared to naked MO at P5, an outcome that is better than any other result published by now. Nevertheless, mice survival did not increase when treated at P7, confirming that the therapeutic window remains a fact. In fact, mice treated with CPPs-MO at P7 showed no increase in survival compared to naked MO, or even scr-treated mice. Therefore, the therapeutic window can be enlarged by the use of CPPs, but SMA treatment and phenotype recovery is not possible after a certain timing, that in our mice is P7 and in humans it still needs to be clarified.

Survival extension after CPP-MO treatment showed a median of 42 days in r6-MO and 23 days in RXR-MO mice. In CPP-treated groups, 37% of r6-MO-treated animals survived to over 3 months of age, and 25% to over 4 months. Overall, r6-MO proved to be superior to RXR-MO in terms of survival, histopathology, and function. For all treatments, an inter-individual

variation was detected in the response to systemic injection, likely resulting from the type of administration. Anyway, these results could represent a huge improvement in clinical practice and a fill in the gap of treatment for symptomatic, adult and mild SMA patients that cannot totally benefit from available therapies, since the diagnosis usually arrives after the first symptoms have shown up. Moreover, SMA is sometimes difficult to diagnose, as symptoms can resemble other conditions or medical problems: usually the patient waits until muscle weakness and decreased muscle tone appear, and by that time it is too late to achieve a complete rescue of the phenotype.

In clinical practice, based on the demonstrated narrow therapeutic window, new-born or maternal screening programmes for SMA could be a possible solution: in some parts of the US new-born babies are now routinely screened for SMA. In Italy a pilot program recently started in Lazio and Toscana with the same aim. This could help performing early treatments, but on the other hand, practical and ethical concerns must be considered before its application: for instance, which cases can be initiated the treatment in utero or immediately after birth? Which treatment should be used? The prediction of the phenotype in cases of different copy number of *SMN2* is not certain. Then, remains unknown how available treatments could act on mild form of SMA and which is their long-term safety and effectiveness.

Besides the effect on survival, we also tested the improvement of the neuropathological phenotype evaluating MN number, NMJ innervation, post-synaptic areas and spinal cord gliosis, and a significant rescue of phenotype occurred in mice treated at P5. In treated mice, motor skill recovery began around P7, in line with histology showing progress at P10. CPPs-MO treated animals maintained motor functions until death, which occurred suddenly

without any evident degeneration. Symptomatic mice treated with CPP-MO conjugates, in comparison with the naked MO, showed improved numbers of innervated NMJs and MNs at P10, as well as increased NMJ synaptic area, and this improvement was maintained up to P30 -and beyond, considering survival and motor ability analyses. This demonstrates that even when symptoms already occurred, live MNs can be protected from death. NMJs seemed to benefit more from the treatment than MNs. NMJ and MN development are strongly linked, though this connection is not well defined. NMJs are an early pathological target in MN diseases [84], since SMN protein present in the CNS has a role in their formation and innervation [74]. We can speculate that treatment with a CPP-MO, given its increased cell distribution, can more efficiently reverse the deficiency of SMN in spare MNs, protecting and preventing their death even in symptomatic stages. Surviving MNs could then re-innervate NMJs. Our treatment can stabilize SMN levels and produce normal-appearing NMJ histology in mice up to P30 and beyond, bypassing the developmental period of major SMN requirement. In rodent models of SMA type 1, multiple synaptic deficits in the neuromuscular units, including NMJ dysfunction and morphological alterations and central proprioceptive sensory synapses onto MNs have been reported [85]. These synaptic defects precede MN loss and the consequent irreversible motor function demise associated with this late event and may represent the biological basis for functional rescue early in symptomatic disease. It is likely that such cellular dysfunction and cellular loss are also intertwined in humans. Furthermore, improvement in NMJ innervation is correlated to decreased muscle atrophy and consequent amelioration of performance in functional tests.

Another aspect we considered is gliosis, which is reported to be associated with areas of MN degeneration in the spinal cord and brain stem

in all three types of human SMA, and recent studies suggest that it contributes to MN death [86]. Our analyses revealed a strong decrease in GFAP-positive astrocyte numbers in spinal cords of CPP-MO mice compared with scr-MO mice, but not compared with naked MO mice.

Our results confirmed the higher effectiveness of the conjugates CPPs-MO into the amelioration of the disease damages even when administered in the symptomatic phase of the disease. This means, if translated to clinics, that could be possible to treat symptomatic patients obtaining a significative amelioration also of the pathological hallmarks if compared to the unconjugated ASO treatments.

An important aspect to be considered when using peptides in clinic is the toxicity profile: it has been demonstrated that the easier passage across the membrane mediated by the CPP conjugation could result in toxic effects mainly related to membrane perturbation. It was also evidenced that the toxicity profiles are different for each CPP, depending on chemistry, dose and/or frequency of administration and route of administration [87]. In addition, in some cases the conjugated compound results to be more toxic than the CPP or MO administered alone [63]. Recent studies demonstrated that the ameliorated biodistribution mediated by CPP conjugation can allow to further reduce the dose of conjugated MO minimizing the toxic effects [58]. The dosage that we selected, based on previous experiments conducted in our laboratory (12 nmoles/g), is the highest we tested, but the only one to have a real effect on treated animals: interestingly, this did not lead to higher toxicity or side effects, and liver and kidney enzymes analysis did not reveal any aberration after treatment, suggesting that our compounds are not toxic at all. Hua et al. [75], highlighted the necessity of peripheral SMN restoration for a complete rescue of SMA pathology in mouse model, and Hensel *et al.* have

suggested that peripheral SMN restoration may be needed, complementing SMN restoration in the CNS [88]. To collect data about MO biodistribution with and without conjugation to a CPP, we adapted a specific ELISA protocol [69] to detect our MO oligomer, obtaining an innovative method that could be useful in determining the exact effective dose to be administered towards clinical perspective. We found remarkable amounts of MO in peripheral organs, in particular in liver and heart, suggesting that systemic IP injection promoted dispersion of the conjugate, probably due to the peritoneum's distance from the brain and spinal cord and its proximity to the liver. In the future, it would be interesting to explore the efficacy of subcutaneous injection, another systemic delivery, to compare the exact required dose. In our work, we used IP delivery for practical reasons in mice, while in humans intravenous injection will be the most likely route of administration, which is less invasive compared to the intrathecal injection used for Nusinersen, ameliorating the compliance.

A possible way to enhance the action of CPPs-MO could be the double administration of the compounds, in a way that was possible lowering the dosage administered for each injection [58]. For unconjugated ASO, Hua et al. performed a double administration of ASO in P0 and P3 mice ICV or SC, and demonstrated a significative elongation of the survival in mice treated with a double dose compared to the single one. Also, Porensky *et al* [89]tested a double administration at P0 and P30 but with no difference in survival compared to a single injection.

Another approach that is sometimes used in SMA preclinical studies is the treatment during pregnancy, a way to administer the therapeutic compound as soon as possible to the affected mice. On this regard, promising results with gene therapy administered in SMA fetal rodents were obtained [90].

Obviously, this approach is still tricky from both the technical and the clinical point of view.

Several studies have demonstrated that IGF1 have a trophic effect on neuronal regeneration and stimulates protein synthesis in neurons and glia [91]. Disruption of the *IGF1* system has been described in neurodegenerative diseases, including Alzheimer's disease, amyotrophic lateral sclerosis, and SMA [92]. All SMA mice exhibit reduced body weight, and since the liver is the major organ that produces *IGF1*, which modulates animal growth, Hua et al. examined serum levels, that were significantly reduced compared to heterozygous controls [93]. However, the expression of IGF-binding protein acid-labile subunit (*IGFALS*) was also affected in SMA mice [75]. Moreover, increasing SMN levels by ASO treatment is reported to re-establish this system [58,75]. Since *IGFALS* expression correlated with *SMN* deficiency, it is possible that early deficiency in circulating *IGF1* may contribute to SMA pathogenesis: in fact, local increases in *IGF1* in either the spinal cord or muscle increase the survival of mice with severe SMA [94]. Mice that do not express *IGF1* are also phenotypically similar to SMA mice, exhibiting a similar small size, severe muscle dystrophy, and early death [75]. We tested both *IGF1* and *IGFALS* in WT and SMA mice: liver expression levels of both genes decreased markedly in SMA compared with unaffected mice. Only *IGF1* expression could be rescued by CPP-MO treatment, making more experiments necessary to clarify the mechanism of action and the correlation between *SMN* and *IGF1* system expression.

Overall, we demonstrated that the two conjugates, in particular r6-MO, were able to reach the CNS in mice at P5 after IP injection. This avoided invasive intrathecal injection and improved SMN levels and consequently SMA symptoms compared with the naked MO, a novel result in SMA mice.

Since symptomatic SMA patients and late-onset mild SMA patients are currently the most difficult to treat, our conjugate should be considered a great improvement from a clinical perspective. Based on the results we obtained, we believe strongly in the feasibility of clinical translation and the utility of the CPP-MO conjugates, even in symptomatic SMA patients.

# BIBLIOGRAPHY


[1] S. Ogino, D.G.B. Leonard, H. Rennert, W.J. Ewens, R.B. Wilson, Genetic risk assessment in carrier testing for spinal muscular atrophy, Am. J. Med. Genet. 110 (2002) 301–307. https://doi.org/10.1002/ajmg.10425.

[2] S. Lefebvre, L. Bürglen, S. Reboullet, O. Clermont, P. Burlet, L. Viollet, B. Benichou, C. Cruaud, P. Millasseau, M. Zeviani, D. Le Paslier, J. Frézal, D. Cohen, J. Weissenbach, A. Munnich, J. Melki, Identification and characterization of a spinal muscular atrophy-determining gene, Cell. 80 (1995) 155–165. https://doi.org/10.1016/0092-8674(95)90460-3.

[3] P. d'Errico, M. Boido, A. Piras, V. Valsecchi, E. De Amicis, D. Locatelli, S. Capra, F. Vagni, A. Vercelli, G. Battaglia, Selective Vulnerability of Spinal and Cortical Motor Neuron Subpopulations in delta7 SMA Mice, PLoS ONE. 8 (2013) e82654. https://doi.org/10.1371/journal.pone.0082654.

[4] M. Boido, A. Vercelli, Neuromuscular Junctions as Key Contributors and Therapeutic Targets in Spinal Muscular Atrophy, Front. Neuroanat. 10 (2016). https://doi.org/10.3389/fnana.2016.00006.

[5] W.D. Arnold, D. Kassar, J.T. Kissel, Spinal muscular atrophy: Diagnosis and management in a new therapeutic era: Spinal Muscular Atrophy, Muscle Nerve. 51 (2015) 157–167. https://doi.org/10.1002/mus.24497.

[6] T.L. Munsat, K.E. Davies, International SMA Consortium Meeting (26–28 June 1992, Bonn, Germany), Neuromuscul. Disord. 2 (1992) 423–428. https://doi.org/10.1016/S0960-8966(06)80015-5.

[7] M.A. Farrar, M.C. Kiernan, The Genetics of Spinal Muscular Atrophy: Progress and Challenges, Neurotherapeutics. 12 (2015) 290–302. https://doi.org/10.1007/s13311-014-0314-x.

[8] A. Ramirez, PEPTIDE-CONJUGATED MORPHOLINO OLIGOMERS FOR TREATMENT OF SPINAL MUSCULAR ATROPHY, (n.d.) 124.

[9] U.R. Monani, A single nucleotide difference that alters splicing patterns distinguishes the SMA gene SMN1 from the copy gene SMN2, Hum. Mol. Genet. 8 (1999) 1177–1183. https://doi.org/10.1093/hmg/8.7.1177.

[10] C. Rochette, N. Gilbert, L. Simard, SMN gene duplication and the emergence of the SMN2 gene occurred in distinct hominids: SMN2 is unique to Homo sapiens, Hum. Genet. 108 (2001) 255–266. https://doi.org/10.1007/s004390100473.

[11] M.E.R. Butchbach, Copy Number Variations in the Survival Motor Neuron Genes: Implications for Spinal Muscular Atrophy and Other Neurodegenerative Diseases, Front. Mol. Biosci. 3 (2016). https://doi.org/10.3389/fmolb.2016.00007.

[12] S. Rudnik-Schöneborn, C. Berg, K. Zerres, C. Betzler, T. Grimm, T. Eggermann, K. Eggermann, R. Wirth, B. Wirth, R. Heller, Genotype-phenotype studies in

infantile spinal muscular atrophy (SMA) type I in Germany: implications for clinical trials and genetic counselling, Clin. Genet. 76 (2009) 168–178. https://doi.org/10.1111/j.1399-0004.2009.01200.x.
[13] T.W. Prior, K.J. Swoboda, H.D. Scott, A.Q. Hejmanowski, HomozygousSMN1 deletions in unaffected family members and modification of the phenotype bySMN2, Am. J. Med. Genet. 130A (2004) 307–310. https://doi.org/10.1002/ajmg.a.30251.
[14] L. Bürglen, S. Lefebvre, O. Clermont, P. Burlet, L. Viollet, C. Cruaud, A. Munnich, J. Melki, Structure and Organization of the Human Survival Motor Neurone (SMN) Gene, Genomics. 32 (1996) 479–482. https://doi.org/10.1006/geno.1996.0147.
[15] L. Cartegni, M.L. Hastings, J.A. Calarco, E. de Stanchina, A.R. Krainer, Determinants of Exon 7 Splicing in the Spinal Muscular Atrophy Genes, SMN1 and SMN2, Am. J. Hum. Genet. 78 (2006) 63–77. https://doi.org/10.1086/498853.
[16] T. Kashima, J.L. Manley, A negative element in SMN2 exon 7 inhibits splicing in spinal muscular atrophy, Nat. Genet. 34 (2003) 460–463. https://doi.org/10.1038/ng1207.
[17] N.K. Singh, N.N. Singh, E.J. Androphy, R.N. Singh, Splicing of a Critical Exon of Human *Survival Motor Neuron* Is Regulated by a Unique Silencer Element Located in the Last Intron, Mol. Cell. Biol. 26 (2006) 1333–1346. https://doi.org/10.1128/MCB.26.4.1333-1346.2006.
[18] T. Kashima, N. Rao, C.J. David, J.L. Manley, hnRNP A1 functions with specificity in repression of SMN2 exon 7 splicing, Hum. Mol. Genet. 16 (2007) 3149–3159. https://doi.org/10.1093/hmg/ddm276.
[19] J. Vitte, C. Fassier, F.D. Tiziano, C. Dalard, S. Soave, N. Roblot, C. Brahe, P. Saugier-Veber, J.P. Bonnefont, J. Melki, Refined Characterization of the Expression and Stability of the SMN Gene Products, Am. J. Pathol. 171 (2007) 1269–1280. https://doi.org/10.2353/ajpath.2007.070399.
[20] H. Chaytow, Y.-T. Huang, T.H. Gillingwater, K.M.E. Faller, The role of survival motor neuron protein (SMN) in protein homeostasis, Cell. Mol. Life Sci. 75 (2018) 3877–3894. https://doi.org/10.1007/s00018-018-2849-1.
[21] F. Gabanella, M.E.R. Butchbach, L. Saieva, C. Carissimi, A.H.M. Burghes, L. Pellizzoni, Ribonucleoprotein Assembly Defects Correlate with Spinal Muscular Atrophy Severity and Preferentially Affect a Subset of Spliceosomal snRNPs, PLoS ONE. 2 (2007) e921. https://doi.org/10.1371/journal.pone.0000921.
[22] Z. Spiró, A. Koh, S. Tay, K. See, C. Winkler, Transcriptional enhancement of Smn levels in motoneurons is crucial for proper axon morphology in zebrafish, Sci. Rep. 6 (2016) 27470. https://doi.org/10.1038/srep27470.

[23] B. Schrank, R. Gotz, J.M. Gunnersen, J.M. Ure, K.V. Toyka, A.G. Smith, M. Sendtner, Inactivation of the survival motor neuron gene, a candidate gene for human spinal muscular atrophy, leads to massive cell death in early mouse embryos, Proc. Natl. Acad. Sci. 94 (1997) 9920–9925. https://doi.org/10.1073/pnas.94.18.9920.
[24] H.M. Hsieh-Li, J.-G. Chang, Y.-J. Jong, M.-H. Wu, N.M. Wang, C.H. Tsai, H. Li, A mouse model for spinal muscular atrophy, Nat. Genet. 24 (2000) 66–70. https://doi.org/10.1038/71709.
[25] U.R. Monani, M.T. Pastore, T.O. Gavrilina, S. Jablonka, T.T. Le, C. Andreassi, J.M. DiCocco, C. Lorson, E.J. Androphy, M. Sendtner, M. Podell, A.H.M. Burghes, A transgene carrying an A2G missense mutation in the SMN gene modulates phenotypic severity in mice with severe (type I) spinal muscular atrophy, J. Cell Biol. 160 (2003) 41–52. https://doi.org/10.1083/jcb.200208079.
[26] T.T. Le, L.T. Pham, M.E.R. Butchbach, H.L. Zhang, U.R. Monani, D.D. Coovert, T.O. Gavrilina, L. Xing, G.J. Bassell, A.H.M. Burghes, SMNΔ7, the major product of the centromeric survival motor neuron (SMN2) gene, extends survival in mice with spinal muscular atrophy and associates with full-length SMN, Hum. Mol. Genet. 14 (2005) 845–857. https://doi.org/10.1093/hmg/ddi078.
[27] T.T. Le, L.T. Pham, M.E.R. Butchbach, H.L. Zhang, U.R. Monani, D.D. Coovert, T.O. Gavrilina, L. Xing, G.J. Bassell, A.H.M. Burghes, SMNΔ7, the major product of the centromeric survival motor neuron (SMN2) gene, extends survival in mice with spinal muscular atrophy and associates with full-length SMN, Hum. Mol. Genet. 14 (2005) 845–857. https://doi.org/10.1093/hmg/ddi078.
[28] T. Gidaro, L. Servais, Nusinersen treatment of spinal muscular atrophy: current knowledge and existing gaps, Dev. Med. Child Neurol. 61 (2019) 19–24. https://doi.org/10.1111/dmcn.14027.
[29] S. Messina, M. Sframeli, L. Maggi, A. D'Amico, C. Bruno, G. Comi, E. Mercuri, Spinal muscular atrophy: state of the art and new therapeutic strategies, Neurol. Sci. (2021). https://doi.org/10.1007/s10072-021-05258-3.
[30] https://www.spinraza.com/, (n.d.).
[31] R.S. Finkel, C.A. Chiriboga, J. Vajsar, J.W. Day, J. Montes, D.C. De Vivo, M. Yamashita, F. Rigo, G. Hung, E. Schneider, D.A. Norris, S. Xia, C.F. Bennett, K.M. Bishop, Treatment of infantile-onset spinal muscular atrophy with nusinersen: a phase 2, open-label, dose-escalation study, The Lancet. 388 (2016) 3017–3026. https://doi.org/10.1016/S0140-6736(16)31408-8.
[32] E. Mercuri, Spinal muscular atrophy — insights and challenges in the treatment era, (n.d.) 10.

[33] D. Stevens, M.K. Claborn, B.L. Gildon, T.L. Kessler, C. Walker, Onasemnogene Abeparvovec-xioi: Gene Therapy for Spinal Muscular Atrophy, Ann. Pharmacother. 54 (2020) 1001–1009. https://doi.org/10.1177/1060028020914274.
[34] A. Poirier, M. Weetall, K. Heinig, F. Bucheli, K. Schoenlein, J. Alsenz, S. Bassett, M. Ullah, C. Senn, H. Ratni, N. Naryshkin, S. Paushkin, L. Mueller, Risdiplam distributes and increases SMN protein in both the central nervous system and peripheral organs, Pharmacol. Res. Perspect. 6 (2018) e00447. https://doi.org/10.1002/prp2.447.
[35] C. Sunyach, M. Michaud, T. Arnoux, N. Bernard-Marissal, J. Aebischer, V. Latyszenok, C. Gouarné, C. Raoul, R.M. Pruss, T. Bordet, B. Pettmann, Olesoxime delays muscle denervation, astrogliosis, microglial activation and motoneuron death in an ALS mouse model, Neuropharmacology. 62 (2012) 2346–2353. https://doi.org/10.1016/j.neuropharm.2012.02.013.
[36] G.E. Oprea, S. Kröber, M.L. McWhorter, W. Rossoll, S. Müller, M. Krawczak, G.J. Bassell, C.E. Beattie, B. Wirth, Plastin 3 Is a Protective Modifier of Autosomal Recessive Spinal Muscular Atrophy, Science. 320 (2008) 524–527. https://doi.org/10.1126/science.1155085.
[37] M. Riessland, A. Kaczmarek, S. Schneider, K.J. Swoboda, H. Löhr, C. Bradler, V. Grysko, M. Dimitriadi, S. Hosseinibarkooie, L. Torres-Benito, M. Peters, A. Upadhyay, N. Biglari, S. Kröber, I. Hölker, L. Garbes, C. Gilissen, A. Hoischen, G. Nürnberg, P. Nürnberg, M. Walter, F. Rigo, C.F. Bennett, M.J. Kye, A.C. Hart, M. Hammerschmidt, P. Kloppenburg, B. Wirth, Neurocalcin Delta Suppression Protects against Spinal Muscular Atrophy in Humans and across Species by Restoring Impaired Endocytosis, Am. J. Hum. Genet. 100 (2017) 297–315. https://doi.org/10.1016/j.ajhg.2017.01.005.
[38] E. Janzen, N. Mendoza-Ferreira, S. Hosseinibarkooie, S. Schneider, K. Hupperich, T. Tschanz, V. Grysko, M. Riessland, M. Hammerschmidt, F. Rigo, C.F. Bennett, M.J. Kye, L. Torres-Benito, B. Wirth, CHP1 reduction ameliorates spinal muscular atrophy pathology by restoring calcineurin activity and endocytosis, Brain. 141 (2018) 2343–2361. https://doi.org/10.1093/brain/awy167.
[39] S. Corti, M. Nizzardo, C. Simone, M. Falcone, M. Nardini, D. Ronchi, C. Donadoni, S. Salani, G. Riboldi, F. Magri, G. Menozzi, C. Bonaglia, F. Rizzo, N. Bresolin, G.P. Comi, Genetic Correction of Human Induced Pluripotent Stem Cells from Patients with Spinal Muscular Atrophy, Sci. Transl. Med. 4 (2012). https://doi.org/10.1126/scitranslmed.3004108.
[40] A. Govoni, D. Gagliardi, G.P. Comi, S. Corti, Time Is Motor Neuron: Therapeutic Window and Its Correlation with Pathogenetic Mechanisms in Spinal Muscular Atrophy, Mol. Neurobiol. 55 (2018) 6307–6318. https://doi.org/10.1007/s12035-017-0831-9.

[41] B.A. Perez, A. Shutterly, Y.K. Chan, B.J. Byrne, M. Corti, Management of Neuroinflammatory Responses to AAV-Mediated Gene Therapies for Neurodegenerative Diseases, (2020) 16.
[42] H. Chaytow, K.M.E. Faller, Y.-T. Huang, T.H. Gillingwater, Spinal muscular atrophy: From approved therapies to future therapeutic targets for personalized medicine, Cell Rep. Med. 2 (2021) 100346. https://doi.org/10.1016/j.xcrm.2021.100346.
[43] J. Summerton, D. Weller, Morpholino Antisense Oligomers: Design, Preparation, and Properties, Antisense Nucleic Acid Drug Dev. 7 (1997) 187–195. https://doi.org/10.1089/oli.1.1997.7.187.
[44] K.M. Schoch, T.M. Miller, Antisense Oligonucleotides: Translation from Mouse Models to Human Neurodegenerative Diseases, Neuron. 94 (2017) 1056–1070. https://doi.org/10.1016/j.neuron.2017.04.010.
[45] A.H.M. Burghes, C.E. Beattie, Spinal muscular atrophy: why do low levels of survival motor neuron protein make motor neurons sick?, Nat. Rev. Neurosci. 10 (2009) 597–609. https://doi.org/10.1038/nrn2670.
[46] C. Mitrpant, P. Porensky, H. Zhou, L. Price, F. Muntoni, S. Fletcher, S.D. Wilton, A.H.M. Burghes, Improved Antisense Oligonucleotide Design to Suppress Aberrant SMN2 Gene Transcript Processing: Towards a Treatment for Spinal Muscular Atrophy, PLoS ONE. 8 (2013) e62114. https://doi.org/10.1371/journal.pone.0062114.
[47] M. Nizzardo, C. Simone, S. Salani, M.-D. Ruepp, F. Rizzo, M. Ruggieri, C. Zanetta, S. Brajkovic, H.M. Moulton, O. Müehlemann, N. Bresolin, G.P. Comi, S. Corti, Effect of Combined Systemic and Local Morpholino Treatment on the Spinal Muscular Atrophy Δ7 Mouse Model Phenotype, Clin. Ther. 36 (2014) 340-356.e5. https://doi.org/10.1016/j.clinthera.2014.02.004.
[48] Y. Dang, C. van Heusden, V. Nickerson, F. Chung, Y. Wang, N.L. Quinney, M. Gentzsch, S.H. Randell, H.M. Moulton, R. Kole, A. Ni, R.L. Juliano, S.M. Kreda, Enhanced delivery of peptide-morpholino oligonucleotides with a small molecule to correct splicing defects in the lung, (n.d.) 14.
[49] C.M. Fadzen, R.L. Holden, J.M. Wolfe, Z.-N. Choo, C.K. Schissel, M. Yao, G.J. Hanson, B.L. Pentelute, Chimeras of Cell-Penetrating Peptides Demonstrate Synergistic Improvement in Antisense Efficacy, (2019) 10.
[50] M. Rizzuti, M. Nizzardo, C. Zanetta, A. Ramirez, S. Corti, Therapeutic applications of the cell-penetrating HIV-1 Tat peptide, Drug Discov. Today. 20 (2015) 76–85. https://doi.org/10.1016/j.drudis.2014.09.017.
[51] L. Du, R. Kayali, C. Bertoni, F. Fike, H. Hu, P.L. Iversen, R.A. Gatti, Arginine-rich cell-penetrating peptide dramatically enhances AMO-mediated ATM aberrant splicing correction and enables delivery to brain and cerebellum, Hum. Mol. Genet. 20 (2011) 3151–3160. https://doi.org/10.1093/hmg/ddr217.

[52] R. Abes, A. Arzumanov, H. Moulton, S. Abes, G. Ivanova, M.J. Gait, P. Iversen, B. Lebleu, Arginine-rich cell penetrating peptides: Design, structure–activity, and applications to alter pre-mRNA splicing by steric-block oligonucleotides, J. Pept. Sci. 14 (2008) 455–460. https://doi.org/10.1002/psc.979.
[53] B. Layek, L. Lipp, J. Singh, Cell Penetrating Peptide Conjugated Chitosan for Enhanced Delivery of Nucleic Acid, Int. J. Mol. Sci. 16 (2015) 28912–28930. https://doi.org/10.3390/ijms161226142.
[54] P. Säälik, A. Elmquist, M. Hansen, K. Padari, K. Saar, K. Viht, Ü. Langel, M. Pooga, Protein Cargo Delivery Properties of Cell-Penetrating Peptides. A Comparative Study, Bioconjug. Chem. 15 (2004) 1246–1253. https://doi.org/10.1021/bc049938y.
[55] A. Joliot, A. Prochiantz, Homeoproteins as natural Penetratin cargoes with signaling properties ☆, Adv. Drug Deliv. Rev. (2008) 6.
[56] M. Pooga, C. Kut, M. Kihlmark, M. Hällbrink, S. Fernaeus, R. Raid, T. Land, E. Hallberg, T. Bartfai, Ü. Langel, Cellular translocation of proteins by transportan, FASEB J. 15 (2001) 1451–1453. https://doi.org/10.1096/fj.00-0780fje.
[57] H.M. Moulton, J.D. Moulton, Morpholinos and their peptide conjugates: Therapeutic promise and challenge for Duchenne muscular dystrophy, Biochim. Biophys. Acta BBA - Biomembr. 1798 (2010) 2296–2303. https://doi.org/10.1016/j.bbamem.2010.02.012.
[58] S.M. Hammond, G. Hazell, F. Shabanpoor, A.F. Saleh, M. Bowerman, J.N. Sleigh, K.E. Meijboom, H. Zhou, F. Muntoni, K. Talbot, M.J. Gait, M.J.A. Wood, Systemic peptide-mediated oligonucleotide therapy improves long-term survival in spinal muscular atrophy, Proc. Natl. Acad. Sci. 113 (2016) 10962–10967. https://doi.org/10.1073/pnas.1605731113.
[59] B. Tajik-Ahmadabad, A. Polyzos, F. Separovic, F. Shabanpoor, Amphiphilic lipopeptide significantly enhances uptake of charge-neutral splice switching morpholino oligonucleotide in spinal muscular atrophy patient-derived fibroblasts, Int. J. Pharm. 532 (2017) 21–28. https://doi.org/10.1016/j.ijpharm.2017.08.116.
[60] F. Shabanpoor, S.M. Hammond, F. Abendroth, G. Hazell, M.J.A. Wood, M.J. Gait, Identification of a Peptide for Systemic Brain Delivery of a Morpholino Oligonucleotide in Mouse Models of Spinal Muscular Atrophy, Nucleic Acid Ther. 27 (2017) 130–143. https://doi.org/10.1089/nat.2016.0652.
[61] A. Kerkis, M.A.F. Hayashi, T. Yamane, I. Kerkis, Properties of cell penetrating peptides (CPPs), IUBMB Life. 58 (2006) 7–13. https://doi.org/10.1080/15216540500494508.
[62] B. Wu, H.M. Moulton, P.L. Iversen, J. Jiang, J. Li, J. Li, C.F. Spurney, A. Sali, A.D. Guerron, K. Nagaraju, T. Doran, P. Lu, X. Xiao, Q.L. Lu, Effective rescue

of dystrophin improves cardiac function in dystrophin-deficient mice by a modified morpholino oligomer, (n.d.) 6.
[63] H.M. Moulton, M.H. Nelson, S.A. Hatlevig, M.T. Reddy, P.L. Iversen, Cellular Uptake of Antisense Morpholino Oligomers Conjugated to Arginine-Rich Peptides, Bioconjug. Chem. 15 (2004) 290–299. https://doi.org/10.1021/bc034221g.
[64] C. Foged, H.M. Nielsen, Cell-penetrating peptides for drug delivery across membrane barriers, Expert Opin. Drug Deliv. 5 (2008) 105–117. https://doi.org/10.1517/17425247.5.1.105.
[65] M.E.R. Butchbach, J.D. Edwards, A.H.M. Burghes, Abnormal motor phenotype in the SMNΔ7 mouse model of spinal muscular atrophy, Neurobiol. Dis. 27 (2007) 207–219. https://doi.org/10.1016/j.nbd.2007.04.009.
[66] G.E. Truett, P. Heeger, R.L. Mynatt, A.A. Truett, J.A. Walker, M.L. Warman, Preparation of PCR-Quality Mouse Genomic DNA with Hot Sodium Hydroxide and Tris (HotSHOT), BioTechniques. 29 (2000) 52–54. https://doi.org/10.2144/00291bm09.
[67] K.D. Foust, X. Wang, V.L. McGovern, L. Braun, A.K. Bevan, A.M. Haidet, T.T. Le, P.R. Morales, M.M. Rich, A.H.M. Burghes, B.K. Kaspar, Rescue of the spinal muscular atrophy phenotype in a mouse model by early postnatal delivery of SMN, Nat. Biotechnol. 28 (2010) 271–274. https://doi.org/10.1038/nbt.1610.
[68] V. Arioli, E. Rossi, Errors Related to Different Techniques of Intraperitoneal Injection in Mice, (n.d.) 2.
[69] U. Burki, J. Keane, A. Blain, L. O'Donovan, M.J. Gait, S.H. Laval, V. Straub, Development and Application of an Ultrasensitive Hybridization-Based ELISA Method for the Determination of Peptide-Conjugated Phosphorodiamidate Morpholino Oligonucleotides, Nucleic Acid Ther. 25 (2015) 275–284. https://doi.org/10.1089/nat.2014.0528.
[70] V. Valsecchi, M. Boido, E. De Amicis, A. Piras, A. Vercelli, Expression of Muscle-Specific MiRNA 206 in the Progression of Disease in a Murine SMA Model, PLOS ONE. 10 (2015) e0128560. https://doi.org/10.1371/journal.pone.0128560.
[71] A. DeChick, R. Hetz, J. Lee, D.L. Speelman, Increased Skeletal Muscle Fiber Cross-Sectional Area, Muscle Phenotype Shift, and Altered Insulin Signaling in Rat Hindlimb Muscles in a Prenatally Androgenized Rat Model for Polycystic Ovary Syndrome, Int. J. Mol. Sci. 21 (2020) 7918. https://doi.org/10.3390/ijms21217918.
[72] I. Jalenques, E. Albuisson, G. Despres, R. Romand, Distribution of glial fibrillary acidic protein (GFAP) in the cochlear nucleus of adult and aged rats,

Brain Res. 686 (1995) 223–232. https://doi.org/10.1016/0006-8993(95)00463-Z.
[73] N.R. Saunders, S.A. Liddelow, K.M. Dziegielewska, Barrier Mechanisms in the Developing Brain, Front. Pharmacol. 3 (2012). https://doi.org/10.3389/fphar.2012.00046.
[74] S. Kariya, T. Obis, C. Garone, T. Akay, F. Sera, S. Iwata, S. Homma, U.R. Monani, Requirement of enhanced Survival Motoneuron protein imposed during neuromuscular junction maturation, J. Clin. Invest. 124 (2014) 785–800. https://doi.org/10.1172/JCI72017.
[75] Y. Hua, K. Sahashi, F. Rigo, G. Hung, G. Horev, C.F. Bennett, A.R. Krainer, Peripheral SMN restoration is essential for long-term rescue of a severe spinal muscular atrophy mouse model, Nature. 478 (2011) 123–126. https://doi.org/10.1038/nature10485.
[76] A. D'Amico, E. Mercuri, F.D. Tiziano, E. Bertini, Spinal muscular atrophy, Orphanet J. Rare Dis. 6 (2011) 71. https://doi.org/10.1186/1750-1172-6-71.
[77] K. Talbot, E.F. Tizzano, The clinical landscape for SMA in a new therapeutic era, Gene Ther. 24 (2017) 529–533. https://doi.org/10.1038/gt.2017.52.
[78] Y. Hua, Y.H. Liu, K. Sahashi, F. Rigo, C.F. Bennett, A.R. Krainer, Motor neuron cell-nonautonomous rescue of spinal muscular atrophy phenotypes in mild and severe transgenic mouse models, Genes Dev. 29 (2015) 288–297. https://doi.org/10.1101/gad.256644.114.
[79] Y. Echigoya, K.R.Q. Lim, D. Melo, B. Bao, N. Trieu, Y. Mizobe, R. Maruyama, K. Mamchaoui, J. Tanihata, Y. Aoki, S. Takeda, V. Mouly, W. Duddy, T. Yokota, Exons 45–55 Skipping Using Mutation-Tailored Cocktails of Antisense Morpholinos in the DMD Gene, Mol. Ther. 27 (2019) 2005–2017. https://doi.org/10.1016/j.ymthe.2019.07.012.
[80] S. Abes, H.M. Moulton, P. Clair, P. Prevot, D.S. Youngblood, R.P. Wu, P.L. Iversen, B. Lebleu, Vectorization of morpholino oligomers by the (R-Ahx-R)4 peptide allows efficient splicing correction in the absence of endosomolytic agents, J. Controlled Release. 116 (2006) 304–313. https://doi.org/10.1016/j.jconrel.2006.09.011.
[81] S. Fletcher, K. Honeyman, A.M. Fall, P.L. Harding, R.D. Johnsen, J.P. Steinhaus, H.M. Moulton, P.L. Iversen, S.D. Wilton, Morpholino Oligomer–Mediated Exon Skipping Averts the Onset of Dystrophic Pathology in the mdx Mouse, Mol. Ther. 15 (2007) 1587–1592. https://doi.org/10.1038/sj.mt.6300245.
[82] M.K. Tsoumpra, S. Fukumoto, T. Matsumoto, S. Takeda, M.J.A. Wood, Y. Aoki, Peptide-conjugate antisense based splice-correction for Duchenne muscular dystrophy and other neuromuscular diseases, EBioMedicine. 45 (2019) 630–645. https://doi.org/10.1016/j.ebiom.2019.06.036.

[83] K.M. Kray, V.L. McGovern, D. Chugh, W.D. Arnold, A.H.M. Burghes, Dual SMN inducing therapies can rescue survival and motor unit function in symptomatic Δ7SMA mice, Neurobiol. Dis. 159 (2021) 105488. https://doi.org/10.1016/j.nbd.2021.105488.
[84] Z. Zhang, A.M. Pinto, L. Wan, W. Wang, M.G. Berg, I. Oliva, L.N. Singh, C. Dengler, Z. Wei, G. Dreyfuss, Dysregulation of synaptogenesis genes antecedes motor neuron pathology in spinal muscular atrophy, Proc. Natl. Acad. Sci. 110 (2013) 19348–19353. https://doi.org/10.1073/pnas.1319280110.
[85] H.K. Shorrock, T.H. Gillingwater, E.J.N. Groen, Molecular Mechanisms Underlying Sensory-Motor Circuit Dysfunction in SMA, Front. Mol. Neurosci. 12 (2019) 59. https://doi.org/10.3389/fnmol.2019.00059.
[86] E. Abati, G. Citterio, N. Bresolin, G.P. Comi, S. Corti, Glial cells involvement in spinal muscular atrophy: Could SMA be a neuroinflammatory disease?, Neurobiol. Dis. 140 (2020) 104870. https://doi.org/10.1016/j.nbd.2020.104870.
[87] K. Saar, M. Lindgren, M. Hansen, E. Eiríksdóttir, Y. Jiang, K. Rosenthal-Aizman, M. Sassian, Ü. Langel, Cell-penetrating peptides: A comparative membrane toxicity study, Anal. Biochem. 345 (2005) 55–65. https://doi.org/10.1016/j.ab.2005.07.033.
[88] N. Hensel, S. Kubinski, P. Claus, The Need for SMN-Independent Treatments of Spinal Muscular Atrophy (SMA) to Complement SMN-Enhancing Drugs, Front. Neurol. 11 (2020) 45. https://doi.org/10.3389/fneur.2020.00045.
[89] P.N. Porensky, C. Mitrpant, V.L. McGovern, A.K. Bevan, K.D. Foust, B.K. Kaspar, S.D. Wilton, A.H.M. Burghes, A single administration of morpholino antisense oligomer rescues spinal muscular atrophy in mouse, Hum. Mol. Genet. 21 (2012) 1625–1638. https://doi.org/10.1093/hmg/ddr600.
[90] R. Karda, S.M.K. Buckley, C.N. Mattar, J. Ng, G. Massaro, M.P. Hughes, M.A. Kurian, J. Baruteau, P. Gissen, J.K.Y. Chan, C. Bacchelli, S.N. Waddington, A.A. Rahim, Perinatal systemic gene delivery using adeno-associated viral vectors, Front. Mol. Neurosci. 7 (2014). https://doi.org/10.3389/fnmol.2014.00089.
[91] V. Bianchi, V. Locatelli, L. Rizzi, Neurotrophic and Neuroregenerative Effects of GH/IGF1, Int. J. Mol. Sci. 18 (2017) 2441. https://doi.org/10.3390/ijms18112441.
[92] J.L. Trejo, E. Carro, E. Garcia-Galloway, I. Torres-Aleman, Role of insulin-like growth factor I signaling in neurodegenerative diseases, J. Mol. Med. 82 (2004) 156–162. https://doi.org/10.1007/s00109-003-0499-7.
[93] J.-K. Yee, R.-J. Lin, Antisense Oligonucleotides Shed New Light on the Pathogenesis and Treatment of Spinal Muscular Atrophy, Mol. Ther. 20 (2012) 8–10. https://doi.org/10.1038/mt.2011.275.

[94] M. Bosch-Marcé, C.D. Wee, T.L. Martinez, C.E. Lipkes, D.W. Choe, L. Kong, J.P. Van Meerbeke, A. Musarò, C.J. Sumner, Increased IGF-1 in muscle modulates the phenotype of severe SMA mice, Hum. Mol. Genet. 20 (2011) 1844–1853. https://doi.org/10.1093/hmg/ddr067.

# ACKNOWLEDGMENTS

I wish to thank Professor Stefania Corti for the opportunity to join her laboratory. I also wish to thank Dr. Monica Nizzardo for her constant support and the help and precious guide given while supervising my PhD work. A big thank you to all the colleagues I met during this journey and to all the external collaborators that made this work possible.